

SCHEDULING FOR NEXT ERA OPERATIONS
OF GEODETIC VLBI - SIMULATIONS WITH
THE AUSCOPE ARRAY

Elizabeth J. Iles

School Natural Sciences
Department of Mathematics and Physics

Submitted in fulfillment of the requirements for the Master of
Science (Research), University of Tasmania
October 2, 2018

Primary Supervisor: Dr. Lucia McCallum
Supervisor: Dr. Jim Lovell



Statements and Declaration

This thesis contains no material which has been accepted for a degree or diploma by the University or any other institution, except by way of background information and duly acknowledged in the thesis, and to the best of my knowledge and belief no material previously published or written by another person except where due acknowledgement is made in the text of the thesis, nor does the thesis contain any material that infringes copyright.

The publishers of the papers comprising any part of this thesis hold the copyright for that content and access to the material should be sought from the respective journals. The remaining non published content of the thesis may be made available for loan and limited copying and communication in accordance with the Copyright Act 1968.

Acknowledgements

There are so many people that without whom, this thesis and the work behind it, would not have been possible. I wish to thank and acknowledge them all. Some particularly important contributors I've listed here. Lucia, Jim, Jamie, Karen and all the other staff and students in the department. Mum, Ella, Andy, Alex, Laura, Pat, Nic, Mawson, Katsu, Meg and all my other friends and relations who've put up with me these two years. Your support has been invaluable.

Abstract

The technique of Very Long Baseline Interferometry (VLBI) is an important method for the collection of geodetic and astrometric data. At least two telescopes simultaneously observe signals from a range of extra-galactic radio sources, coordinated by a well-optimised observing schedule. Improving this scheduling process is an important focus as we move into the next generation of geodetic VLBI. This project considered Earth Orientation Parameters (EOPs) and station coordinates, in order to develop our understanding of the capabilities and limitations of the traditional scheduling method, as well as the new, automated scheduling mode ‘dynamic scheduling’. Scheduling with the Australian AuScope VLBI array, in particular, was considered through a regime of repeated scheduling, simulation and analysis. However, the findings are widely applicable to other stations and networks hoping to maximise their effective operations in line with the global goals of the geodetic community.

We find that short interruptions to a standard 24 hour schedule will not significantly impact the precision of results. This is true even if the total time lost is up to half the total observing time. Conversely, reducing the length of the observing period results in an exponential-like degradation of precision. The dynamic scheduling mode is shown to be capable of producing results consistent with current scheduling. However, it is significantly more flexible, with close to real-time adaptability. It is shown that the baseline-limited AuScope array can also be augmented dynamically to improve EOP precision through an intermittent contribution from only 2 additional global stations. The results presented here confirm that a positive impact on efficiency and precision in geodetic VLBI can be achieved through effective scheduling. In light of this, the current scheduling practice can be adapted immediately for greater operational capability.

Contents

1	Introduction	1
1.1	This Project	1
1.2	Justification	2
2	Background	5
2.1	Geodetic VLBI	5
2.1.1	Theory and Experimental Details	7
2.1.2	Scientific Applications	13
2.1.3	A Governing Body: IVS	16
2.2	Scheduling Theory and VieVS	17
2.2.1	Scheduling for Operation	18
2.2.2	Scheduling Priorities for Geodetic VLBI	20
2.2.3	Software: VieVS	23
2.3	Next-Generation Aims: VGOS	25
2.3.1	VGOS and its Intended Outcomes	26
2.3.2	Primary Areas of Concern	29
2.4	The AuScope VLBI Network	31
2.4.1	Technical Details	31
2.4.2	Formation	35
2.4.3	Present Operations: AUSTRAL	37
2.4.4	Future Goals	39
3	Traditional Scheduling Method	42

3.1	Simulation Parameters	43
3.2	Decreasing Duration Simulations	44
3.2.1	Earth Orientation Parameters (EOPs)	45
3.2.2	Station Coordinates	47
3.3	Interrupted Scheduling Simulations	50
3.3.1	Creating the ‘Cut’ Schedules	52
3.3.2	EOP and Baseline Repeatability Results	53
3.3.3	Is the Type of Interruption Related to a Greater Effect on Results?	56
4	The Dynamic Scheduler	60
4.1	How Dynamic Scheduling Works	61
4.2	Considering the ‘Update Interval’	65
4.2.1	Simulation Results - EOPs and Baseline Repeatabilities .	66
4.2.2	Variation of Precision with Dynamic Scheduling	69
4.3	Quality Check	73
4.3.1	Simulation	73
4.3.2	Observation	75
5	Simulating a Global Network	78
5.1	Creating a Global Network	79
5.2	Augmenting the AuScope Network with Global Stations	82
5.3	Intermittent Contribution of Support	87
6	Conclusion	91
6.1	Revisiting the Project Motivation	91
6.2	Summary of Results	93
6.2.1	Standard Scheduling Mode	93
6.2.2	Dynamic Scheduling Mode	95
6.3	Conclusion and Future Outlook	97

List of Figures

2.1	<i>A simple depiction of VLBI for two stations A and B. A planar wave approaches from a distant radio source. \underline{s}_o represents the unit-vector of this wave. There is some delay τ between when the signal reaches station B and station A as they are separated by a baseline vector \underline{b}.</i>	8
2.2	<i>A simple representation of how the radio signal data is converted into geodetic and astrometric results through a block diagram. The clock is usually a H-maser and the work of a correlator to turn the recorded signal into usable results is complex.</i>	10
2.3	<i>A representation of the global distribution of IVS components. The legend indicates the nature of each component (Schuh and Behrend, 2012).</i>	17
2.4	<i>A typical IVS observing week which consists of three or four 24h sessions and at least one 1h Intensive session every day. To optimize data transport and to avoid weekend 24 hour sessions, the observing week commences on Monday at 17:00UT with an R1. Following each 24 hour session, there is a 30-min break before the subsequent session starts. The concluding R4 session finishes on Friday at 18:30UT. The Intensive sessions are observed by a small number of stations, either in parallel to the 24h sessions or during the weekend time (Nothnagel et al., 2016a).</i>	19

2.5	<i>A representation of the complexity of the optimisation processes involved with scheduling, based on the developments in the Vienna VLBI Software as presented by Schartner (2017)</i>	23
2.6	<i>An example of the VieVS interface. The General Scheduling parameters window is open with the Run tab displayed. This is Version 2.3, although this has since been superseded by Version 3.0.</i>	25
2.7	<i>Predicted total IVS network for 2018 consisting of new VGOS stations, upgraded stations, and legacy S/X network stations. The Voronoi diagram is based on all network stations. Red circles indicate very fast moving telescopes and blue squares, fast moving telescopes. The upgraded legacy telescopes are marked with black triangles and S/X sites without major upgrades with hollow circles (Hase et al., 2012).</i>	27
2.8	<i>The geographical location of new AuScope VLBI array and GNSS infrastructure. The 12 m telescopes are labelled by name and connected by their respective baselines. Filled dots indicate GNSS sites (Lovell et al., 2013).</i>	32
2.9	<i>Representations of the 12m antennas used in the AuScope VLBI array and their main components (Lovell et al., 2013).</i>	34
2.10	<i>Two depictions of station geodetic VLBI activity for the years 2010 and 2015. The blue dots indicate the position of stations on the globe. The size of the dots is proportional to the number of recorded observations in that year. Even in this 5 year period, there is significant increase in the number of Southern Hemisphere observations (Lovell et al., 2017).</i>	36
3.1	<i>ERP results in terms of the standard deviation of the result (denoted by \times) and the mean of the formal error (error bars) for each schedule duration (Iles et al., 2017).</i>	45

3.2	<i>Baseline repeatabilities rms (mm) for all baselines over decreasing time-steps, colour-coded to allow for identification of each of the 3 baselines.</i>	47
3.3	<i>The smooth curves represent the mathematical \sqrt{n} law for each baseline and its number of observations (n). The simulation results are indicated with a \times and joined to make a comparable line plot. The baselines are differentiable by individual dash patterns in both cases.</i>	49
3.4	<i>Baseline repeatabilities rms (mm) for each of the 3 baselines from Figure 3.2. The lines represent the \sqrt{n} law for each baseline and its total number of observations (n) is stated above each bar (Iles et al., 2017).</i>	50
3.5	<i>Diagrammatic representation of missing hours (0-23) and the corresponding Cut ID designation. Black intervals correspond to time which is missing. A thick horizontal line denotes sections where total time removed changes: 6,9,12,15 hrs.</i>	52
3.6	<i>ERP results in terms of the standard deviation of the result (delineated by \times) and the mean of the formal error (error bars) for each interrupted ‘Cut’ schedule.</i>	54
3.7	<i>Baseline repeatabilities for the Hb-Yg baseline over the variety of interrupted schedule test cases. Schedule names correspond to those in Figure 3.5. The dashed line represents the 24h result from the original schedules in Section 3.2</i>	55
3.8	<i>Diagrammatic representation of interruption patterns from Figure 3.5. Baseline lengths rms (mm) are included and colour coded to identify consistency with Section 3.2’s original 24h result. Blue indicates good agreement, yellow and orange some agreement and red, no clear agreement. EOPs are coloured similarly based on the average over all 5 results.(Iles et al., 2017)</i>	56

3.9	<i>Composite plots of schedule pattern attributes against the rms baseline length for the Hb-Yg baseline, as in Figure 3.7. Blue points are schedules which lose time at the start or end of the schedule, red are those that do not. Negative values indicate the interruption is random, while positive values are repeating patterns. The ‘cut4154’ and ‘cut6126’ schedules previously identified, are enclosed in the dashed region.</i>	57
4.1	<i>A flow chart of the scheduling process where standard observing is compared with dynamic observing. Automated processes are highlighted in green, while processes requiring an operator are in blue. A time-line is also included.</i>	62
4.2	<i>An example of the ‘red button’ program which will allow an operator to specify when a participating station will join or leave a dynamically scheduled session (Lovell et al., 2017).</i>	63
4.3	<i>An example of the live page for dynamic observing. The details of the experiment and all participating stations can be quickly identified from this web-based summary page.</i>	63
4.4	<i>A simple schematic of the information flow for dynamic scheduling in an AuScope experiment (Lovell et al., 2017).</i>	64
4.5	<i>Repeatabilities for all baselines over decreasing dynamic interval. For each baseline, dashed horizontal lines denote the 24h result from the original simulations in Section 3.2.</i>	67
4.6	<i>ERP results in terms of the standard deviation of the result (delineated by \times) and the mean of the formal error (error bars) for each schedule duration. This time produced by the dynamic scheduler and with a number of varying update intervals.</i>	68
4.7	<i>The average number of scans and the average number of different sources observed over 24 hours at different dynamic update intervals.</i>	70

4.8	<i>A version of Figure 4.5 to exclude the shortest update intervals. Repeatabilities for all baselines over decreasing dynamic interval. For each baseline, dashed horizontal lines denote the 24h result from the original simulations in Section 3.2 (Iles et al., 2017)</i>	72
4.9	<i>Baseline repeatabilities for all baselines over decreasing time-steps, as in Section 3.2.2. This time produced with the dynamic scheduler. For each baseline, dashed horizontal lines denote the 24h result from the original simulations in Section 3.2.</i>	75
5.1	<i>Geographical locations for test stations in the defined global network. Some baselines are illustrated by a dashed line to highlight improvements to baseline length and thus, global volume.(Iles et al., 2017)</i>	81
5.2	<i>Indicative ERP results for the range of global networks tested with the dynamic scheduler, presented in terms of the standard deviation of the result and the mean of the formal error as in Section 3.2. R1 and R4 results are also simulated for comparison but are not directly comparable due to the sampling rate (Iles et al., 2017).</i>	84
5.3	<i>Diagrammatic representation of Wz observing hours (0-23) created from Figure 3.5 for dynamic observing. The corresponding CutID designation is used to link patterns with Section 3.3. Black intervals correspond to time which is not observed. A thick horizontal line denotes sections where total operational time changes: 18,15,12,9 hrs.</i>	88

5.4 *Indicative ERP results for the range of dynamic interruptions to
Wettzell’s contribution, as tested in terms of the standard devi-
ation of the result and the mean of the formal error in line with
Section 3.2. R1 and R4 results are also simulated for compari-
son but are not directly comparable due to sampling rate. CutID
numbers correspond to Figure 3.8 and Figure 5.3 (Iles et al.,
2017).* 89

List of Tables

4.1	<i>Dynamic scheduling proof-of-concept observation sessions in 2016 (Lovell et al., 2017).</i>	76
5.1	<i>The test network of global stations used for dynamic scheduling simulations and their locations. The AuScope stations are shaded in grey to more clearly identify the additional IVS stations.</i>	80
5.2	<i>Volume of the global network test cases spanned onto the surface of the globe. *- This is the volume of the total network, however, not all stations observed for the entire duration.(Iles et al., 2017)</i>	83

Chapter 1

Introduction

1.1 This Project

The project which is presented in the following thesis, aimed to further develop our understanding of the ways an observation schedule itself can impact the precision of geodetic Very Long Baseline Interferometry (VLBI) results. This was done specifically with a view to improving efficiency and thus, the management of resources in order to prepare for continuous, 24/7 observation capability in the near future.

Continuous observing is an ambitious observing goal which will either push the limits of our current processes or necessitate a new mode of observing entirely. Here, we consider both options through a range of simulated observing sessions. Earth Orientation Parameters (EOPs) and station coordinates are considered as the primary geodetic products for comparison. Improving the quality of geodetic observations made with the Australian AuScope VLBI array is an institutional goal and as such, the AuScope network forms the basis for the majority of this work. However, we note that the findings are widely applicable, particularly for other stations or networks hoping to maximise their effective operations.

In general, this project is comprised of two main avenues of research: maximising output through time-efficiency while using the traditional method of

scheduling; and the development, testing and application of a new automated scheduling mode, ‘dynamic scheduling’, as a part of the wider dynamic observing concept of Lovell et al. (2014). This is presented in the five subsequent chapters as follows: an introduction to the theoretical background; the traditional scheduling method; the dynamic scheduler tool; global applications for dynamic scheduling; and finally, a discussion of this project’s conclusions, results and future possibilities.

The major findings of this project are published in the summary paper by Iles et al. (2017). However, this document has not been included intact in the following, as a great deal of this thesis documents the process and lead up to any published findings. Citations have been made where appropriate and a copy of the manuscript can be found in the appendix for convenience.

1.2 Justification

Geodesy and the development of a global geodetic reference frame are becoming increasingly important to a wider community. This was demonstrated by the recent recognition from the UN General Assembly highlighting the requirement of precise global geodetic data for future sustainability (UN, 2015). As a primary method for collecting such data, geodetic VLBI has also experienced a heightened global awareness. This has been well timed, as the geodetic VLBI community itself aims to transition to a new generation of observation with an order of magnitude improvement in measurement precision, through large-scale technological and procedural improvements.

The International VLBI Service for Geodesy and Astrometry (IVS) is leading geodetic VLBI towards a more flexible and automated method of observation. In particular, this is through its plans for the next-generation network: the VLBI Global Observing System (VGOS) (Hase et al., 2012). VGOS is planned to be a network optimised for the determination of Earth orientation and terrestrial reference frame parameters. It is to be comprised of fast radio

telescopes (up to 12 deg/s) at old and new sites around the world, with high capacity data acquisition systems (up to 32 Gbps) (Petrachenko et al., 2009). These VGOS antennas will transition to a continuous 24/7 observation program in the near future and thus, significantly increase the total number of global geodetic observations for improved results.

However, the planned transition to VGOS poses a variety of problems to the geodetic community in its current state. Not least of which is the problem of the increased pressure that continuous observing will put on individual station resources. This is where increased automation becomes important and often remote operation is proposed as a solution. Although, while this may be feasible in some select cases, for most sites, it is not a viable option (Lovell et al., 2013). So, while the technological improvements of VGOS will allow greater opportunities for increased experimentation and improve the precision of geodetic results in the community, it is still limited by the resources of the smallest institutions in the network.

Through its association with the AuScope program, the University of Tasmania has made the development of geodetic VLBI observing techniques and remote operation an institutional priority and seen significant success in recent years. One area to which this continuous improvement has been attributed is the optimisation of experiment scheduling (Plank et al., 2017). The importance of efficient and well optimised scheduling is not a new concept for any type of scientific observation program. Effective scheduling has been proven to make a significant difference to the precision of results, the time and cost efficiency of a program and the flexibility of a station to adapt to changing conditions. These are all significant priorities for global geodetic VLBI as we move into the next era of observation.

Even VGOS is still limited by the current requirement to schedule each observing session well in advance and coordinate its distribution through the IVS (Lovell et al., 2013). The current practice is for sessions to be scheduled well in advance, usually spanning 24 hours or longer and involving a subset

of all global VLBI stations, based on their yearly commitment offerings to the IVS (Nothnagel et al., 2016a). There is currently no global plan for this process to evolve, despite what may be considered a variety of obvious benefits in doing so. If we consider an automated scheduling process, such as the dynamic scheduling of Lovell et al. (2014), this could very well solve a number of the resource problems posed by the transition to VGOS. Thereby an effective solution is created, without requiring remote operation. In the transition years, it will also allow more seamless drop-ins and outs for stations with multiple commitments or short notice collaborations (Iles et al., 2017).

For the AuScope network specifically, a revisitation of the requirements for scheduling on the whole is currently pertinent since this network often operates as an independently capable array, as well as a part of the IVS-run experiments. Despite this, the antennas are all currently operating less than they could be and as such, it is an institutional aim to increase AuScope observations in addition to, and on top of, the IVS commitments. This will also allow the array to more effectively meet the VGOS transition requirements. We predict that such aims will become even more common as more stations are developed for global geodesy or are required to prepare for continuous observation and the associated levels of data transport. This prediction is supported by the positive responses to the first call for dynamic observing in 2016 from a variety of globally distributed stations. As such, we justify the following consideration of the scheduling process used by AuScope and global networks with the current community-wide climate of change in geodetic VLBI.

Chapter 2

Background

This project strives to build on the knowledge of and processes for effective scheduling developed over many years of geodetic observations worldwide. As such, it requires a thorough understanding of the history, current applications and goals for the future of geodetic VLBI. There is also a need to balance both theoretical and operational priorities which are dependent on a variety of different factors.

In this chapter, the main building blocks for the ideas behind this project are discussed in some depth to provide a solid foundation for the research and corresponding results presented in the chapters that follow. The background in terms of geodetic VLBI, scheduling theory and systems, the VGOS goals and the AuScope network is included.

2.1 Geodetic VLBI

The idea of using VLBI for geodesy was first proposed by the likes of Matveenko et al. in 1965. However, the field fully came into its own when the first observing sessions of the newly developed Mark-3 system (Clark et al., 1985), allowed for high geodetic and astrometric precision to be achievable with standard VLBI equipment (Nothnagel et al., 2016a). Since its inception, the processes involved have been steadily improving, allowing this technique to evolve into a

valid and necessary tool for the estimation of EOPs as well as the realisation of Celestial and Terrestrial Reference Frames (the CRF and TRF) (Petrov et al., 2009). In recent years, geodesy and its applications have become recognised in a range of forums worldwide. For example, even the United Nations General Assembly has recognised the importance of global geodesy for future sustainability in February 2015 (UN, 2015). Geodetic VLBI is an important method for the collection of global, space-geodetic data and is undertaken by a large number of institutions worldwide.

Geodetic VLBI is important for collecting this kind of data as it is the only space-geodetic technique capable of measuring all five EOPs. Particularly, it is unique for the ability to relate the CRF and TRF directly because it is sensitive to the transformation between the two frames and is the only technique to be capable of measuring the earth rotation angle, usually expressed as the difference between astronomical time and atomic time ($UT1-UTC$). This is a widely influential variable for which accurate and regular measurement is necessary for a range of scientific areas (e.g. Haas et al., 2017). However, the reporting of $UT1-UTC$ is not the only unique capability of geodetic VLBI for geodesy and astrometry. It is also important for determining nutation components and positions of compact extra-galactic radio sources, such as quasars (Nothnagel et al., 2016a).

Currently, geodetic VLBI is a necessary tool for monitoring EOPs and station coordinates and maintaining global reference frames. Coordinated by the IVS (discussed in Section 2.1.3), VLBI is able to accurately measure short and long baselines between global stations, even at an intercontinental scale; provide highly precise EOPs; and identify numerous quasar positions to develop an inertial reference frame. It is indisputably a significant contributor to our understanding of global geodesy.

2.1.1 Theory and Experimental Details

In the broadest sense, VLBI is an interferometric technique which relies on two or more radio telescopes working in tandem to record the emissions of radio sources and thus, to determine the cross-power spectrum of the radio signal (Thompson et al., 1987). From such a spectrum, it is then possible to derive a group interferometric delay which is used to determine precise geodetic results (Shapiro and Knight, 1970).

VLBI differs from other forms of interferometry in a number of ways. Although, predominantly, it is through the necessity, or lack thereof, of connections between the elements during observations (Walker, 1989). VLBI is not limited in this way and so, theoretically, it is possible to include any radio telescope with the appropriate components—an atomic frequency standard, phase locked oscillators and appropriate receiving and recording systems—into a VLBI experiment (Thompson et al., 1987). Thus, VLBI is flexible in the geometry of station configuration which has supported its growth to the global network we see today (see Section 2.1.3).

Scientifically, the fundamental purpose of interferometry is to measure the coherence properties of an electromagnetic field and as such, a radio interferometer can be considered as an analogue to Young’s double slit experiment (Thompson et al., 1987). The primary observable in VLBI is the difference in arrival time of the electromagnetic wavefront received at each station (Robertson, 1991). In this case, it is usually the signal emitted from an extragalactic radio source. This is called the geometric delay (Thompson et al., 1987) and it is a particularly desirable quantity to measure since it is dependent only on the most fundamental of physical properties. That is, it is only derived from a realisation of the atomic second and a clock synchronisation convention (Schuh and Behrend, 2012).

Figure 2.1 shows a simple depiction of this scenario. As described by Schuh and Behrend (2012), the planar wavefront propagates along the unit vector \underline{s}_o until it arrives at the two antennas (in this case Station A and Station B). The

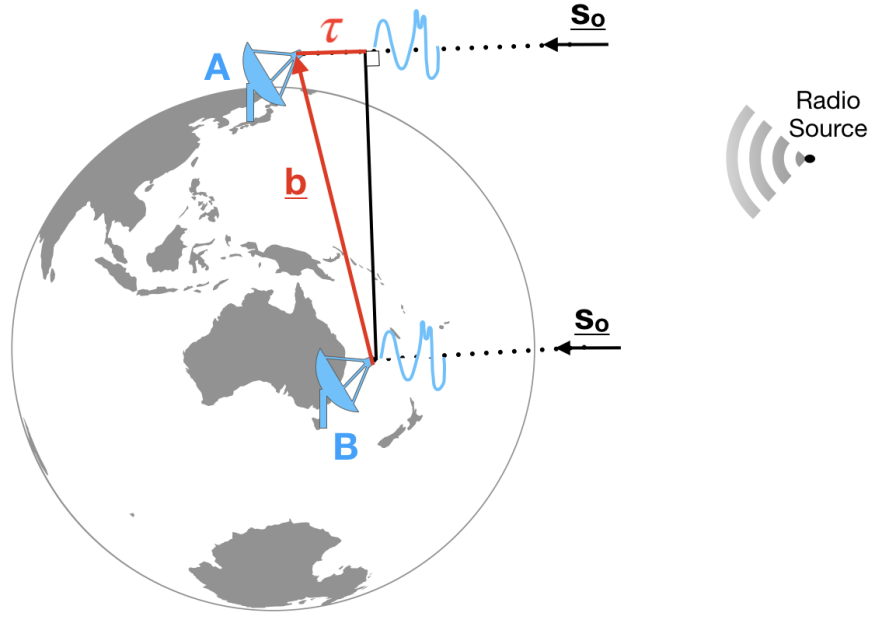


Figure 2.1: A simple depiction of VLBI for two stations A and B. A planar wave approaches from a distant radio source. \underline{s}_o represents the unit-vector of this wave. There is some delay τ between when the signal reaches station B and station A as they are separated by a baseline vector \underline{b} .

stations are separated by the baseline vector \underline{b} . The time delay (geometric delay) is given by the dot product of these two vectors divided by the speed of light. This is described by Equation 2.1, and is one of the most important relationships for geodetic VLBI.

$$\begin{aligned}\tau_g &= \frac{\underline{b} \cdot \underline{s}_o}{c} \\ &= t_B - t_A\end{aligned}\tag{2.1}$$

By measuring this time delay τ_g for many radio sources sequentially and in quick succession, a dataset can be assembled from which it is possible to over-determine the baseline vector and the coordinates of the observed sources (Schuh and Behrend, 2012), as well as to derive the rotational motion of the Earth (Thompson et al., 1987).

In practice, the signal is measured by each station and referenced with electronic signal processing devices, whose time, frequency, and phase information

is derived coherently from an on-site atomic frequency standard, usually a hydrogen maser (Schuh and Behrend, 2012). This measurement involves a convoluted process of amplifying, down-converting and sampling of the signal received from the source, as shown in part by Figure 2.2. The signal is first received at the antenna and amplified using standard radio astronomy equipment. It is mixed with a local oscillator signal derived from the VLBI frequency standard in order to bring one edge of the passband to 0 Hz. Then, the signals are filtered and digitised with sampling, usually at the Nyquist rate (the reciprocal of twice the bandwidth), and over-sampling is often considered to improve the signal-to-noise ratio (SNR) of the data. The data is then formatted and recorded to be sent with the reference information to a correlator (Walker, 1989).

This general measurement process has not changed much, despite VLBI moving into the modern era of observations. However, technological advancements such as increased data storage and transfer rates have greatly impacted the capability of VLBI observations. Correspondingly, the geodetic VLBI techniques used today are many times more accurate than their early predecessors. It is currently common to observe with a multi-band S/X VLBI system, which performs measurements at S band (2.2-2.4 GHz) and X band (8.2-8.95 GHz). This is considered a large frequency range but it too is being labelled as a ‘legacy’ system with the advent of the new broadband delay measurements of the VGOS system, discussed further in Section 2.3 (Schuh and Behrend, 2012).

Once the data has reached the correlator, it is subjected to a cross-correlation process to determine the the best-possible value for τ (Schuh and Behrend, 2012). This is a complex process which involves comparing the signals to a range of trial delays by multiplying the signal with the trial delays until a maximum is reached (Whitney, 2000). This is a process of maximum likelihood estimation, whereby the relative delay at the peak of the cross-correlation function is determined to be the value of the actual delay (Whitney, 2000).

Throughout this process, the correlator must also take into account a num-

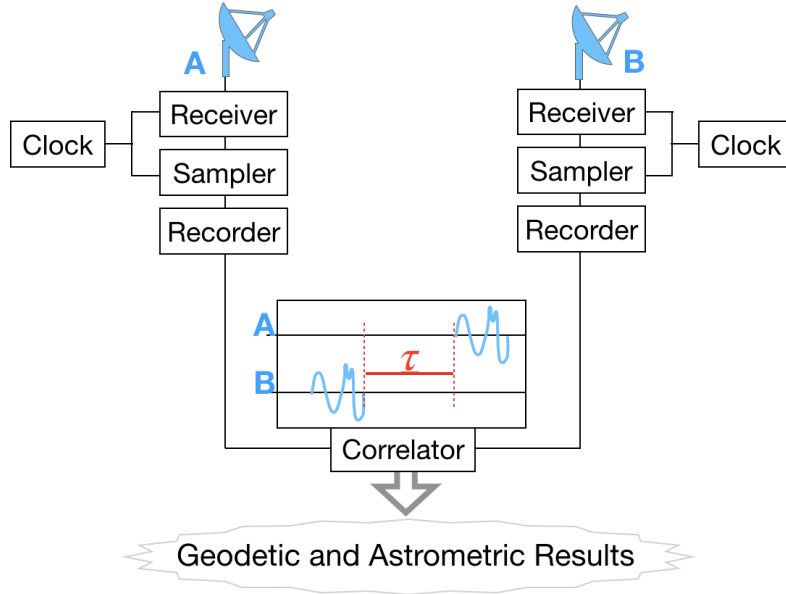


Figure 2.2: *A simple representation of how the radio signal data is converted into geodetic and astrometric results through a block diagram. The clock is usually a H-maser and the work of a correlator to turn the recorded signal into usable results is complex.*

ber of significant Earth rotation effects which will affect station positions over the integration time (Schuh and Behrend, 2012). For example, in the time after reaching the first station but before reaching the second, the Earth (and therefore the second station) will move. Hence, there will be some difference in the additional path length that a planar wavefront must travel to reach the second receiving station, compared to a static-Earth case (Schuh and Behrend, 2012). This is not simply important for determining precise station coordinates but also for source positions through the application of geometry (Thompson et al., 1987).

Hence, the role of a correlator is to read and decode the data; align the streams from each station, accounting for clock offsets and geometric delays; shift the frequency of one data stream on each baseline to account for clock rate offsets and the differential Doppler shift between the stations arising from Earth rotation; multiply each pair of data streams with a range of delays;

thereby, generate a correlation function to determine the results; and finally, write these results to an accessible database for use in geodetic or astrometric purposes (Walker, 1989). This process of taking geodetic data with VLBI is depicted more simply through the flowchart in Figure 2.2.

It is important to note that the signal delay which is measured, is also constrained in precision by the effective bandwidth of the cross-correlated signal and the SNR. This is calculable in the manner described by Equation 2.2. In this case, the SNR is related to the noise observed on the interference fringes and the B_{eff} refers to the effective bandwidth of the recorded VLBI signals (Schuh and Behrend, 2012).

$$\sigma_{\tau} = \frac{1}{2\pi} \cdot \frac{1}{\text{SNR} \cdot B_{eff}} \quad (2.2)$$

As many applications of geodetic VLBI are focused on improving the quality of known quantities, this precision relationship is also particularly significant for geodetic results. In the following chapters, we are particularly interested in improving precision through scheduling, but this would mean nothing if the receiving equipment was imprecise by nature.

With a view to minimising, or at least understanding, the potential errors affecting the main observable of geodetic VLBI (the time delay τ), it is also important to note that, while the signal measured at the correlator is dominated by the geometric delay discussed previously, it also contains a range of contributions from other delay terms. The actual value of τ must be considered as the sum of these delays (see Equation 2.3) and corrected accordingly (Schuh and Behrend, 2012).

$$\tau = \tau_g + \tau_{clk} + \tau_{inst} + \tau_{trop} + \tau_{iono} + \tau_{rel} \quad (2.3)$$

τ_g = the geometric delay

τ_{clk} = a contribution to the signal delay arising from the mis-synchronization of the reference clocks at each observatory

τ_{inst} = a contribution to the signal delay arising from the propagation delays through on-site cable runs and other instrumentation

τ_{trop} = a contribution to the signal delay arising from the propagation delays through the non-ionized portions of the Earth's atmosphere

τ_{iono} = a contribution to the signal delay arising from the propagation delays through the ionized portions of the Earth's atmosphere

τ_{rel} = the special and general relativistic corrections to the classical geometric delay τ_g

For geodetic VLBI, other than the relativistic delay τ_{rel} , these are all small signal delay terms which corrupt the geometric delay and as such, must be accounted for as rigorously as possible. There are a number of techniques to achieve this which are currently used to varying degrees of success. A number of these methods are as follows: computation from known physics for τ_{rel} ; calibration for τ_{inst} ; least squares estimation by modelling, possibly with the aid of locally measured input parameters for τ_{clk} and τ_{trop} ; and a removal based on dual-frequency observations for τ_{iono} (Schuh and Behrend, 2012). This type of correction is also an important part of the geodetic VLBI process for determining precise geodetic and astrometric results (Schuh and Behrend, 2012).

As a final note on the theory of geodetic VLBI, much of the literature refers to this primary observable quantity of VLBI (τ) as a group delay (τ_{gd}) which is determined during the correlation process by fitting a line to a sequence of phases, which have been measured at several discrete frequencies (Schuh and Behrend, 2012). This can be expressed as in Equation 2.4 below.

$$\tau_{gd} = \frac{\delta\phi}{\delta\omega} \quad (2.4)$$

Here, ϕ is the interferometric fringe phase and $\omega = 2\pi\nu$ is the observed angular frequency and as such, the group delay can be said to be the slope

of the frequency-phase relation. Hence, an observable with potentially higher precision would be the phase delay given by Equation 2.5, as it is determined by values rather than a rate of change. However, this relies on the determination of a number of unknown phase cycles and has previously posed an ambiguity problem for geodetic VLBI (Schuh and Behrend, 2012).

$$\tau_{pd} = \frac{\phi}{\omega} \quad (2.5)$$

Therefore, it is usually the group delay which is measured, and applied to geodetic and astrometric uses of VLBI. However, for the next generation of geodetic VLBI (see Section 2.3), a broadband delay is being developed. This is a four-band system that is anticipated to measure four tune-able frequency bands within the entire frequency range of 2 to 14 GHz. In this scenario, the determination of the phase delay should also be an option (Schuh and Behrend, 2012).

2.1.2 Scientific Applications

The previous section outlined the theory and experimental procedures for the measurement and determination of VLBI’s fundamental observable, the time delay. While interesting, this does not particularly lend itself to a simple understanding of how such an observable may be immediately useful. This section briefly addresses the range of applications for current VLBI types of experimentation.

In Section 2.1.1, it was shown that the calibration of baselines and source positions are products of a VLBI observing session and that geodetic data describing the variations in baseline lengths and Earth rotation parameters can be determined by a repetition of these measurements over longer timescales (Thompson et al., 1987). The results obtained from each VLBI session requires the careful estimation of source positions, station coordinates, EOPs, the behaviour of the clock and atmosphere at each antenna location and pre-

cise modelling of a range of geophysical and astronomical effects (Schuh and Behrend, 2012). This is required to determine and produce a number of key scientific outcomes with relevance to a variety of areas, fields and institutions globally.

One such application is in the area of reference frames. In geodesy, these are defined to be the practical realisation of a reference system, formed through observations and consisting of a set of identifiable fiducial points on the plane of reference (i.e. radio sources on the sky, fundamental stations on the Earth’s surface etc.). Wherein, a reference system is the conceptual definition of the coordinates, mathematical and physical attributes, the origin and orientation (Schuh and Behrend, 2012). VLBI is influential in the determination and maintenance of reference frames as it is based on extragalactic objects. In this way, the reference frame is particularly uncomplicated: the universe as a whole does not rotate, and hence, very distant objects cannot have an overall rotational motion (Schuh and Behrend, 2012).

Geodetic VLBI results are used in determining two of the primary global reference frames. In fact, it is the only technique possible for creating and maintaining the International Celestial Reference Frame (ICRF) which is the conventional celestial reference frame catalogue at radio frequencies. For this reference frame, each VLBI session worldwide can contribute a set of relative positions for the observed radio sources. Although this is associated with some uncertainty, over time the uncertainty is reduced, due to the overlap of common sources from one session to another, and therefore, the source positions are determined with increasing precision. For many years, VLBI has been developing the ICRF from the original 608 extragalactic radio sources, of which 212 were defining sources. It was first recognised by the IAU as of 1 January 1998 (Ma, 1999), although the catalogue also relies on observations conducted during the 15 years prior.

As well as determining the ICRF, the extremely precise delay measurements of VLBI are important for the International Terrestrial Reference Frame

(ITRF) which is the conventional terrestrial reference frame. This reference frame is supported by all four space-geodetic techniques. In this capacity, the delay measurements of VLBI sessions are converted from the time domain to metric distances with the speed of light, a conversion factor which is one of the fundamental constants of nature (Schuh and Behrend, 2012).

Geodetic VLBI is also an effective technique for the determination of precession and nutation, polar motion, and universal time, as discussed previously. A large portion of the following chapters focus on improving geodetic precision through a consideration of a number of these quantities. In VLBI, there is a need to translate between the conventional inertial system and the conventional terrestrial system (Schuh and Behrend, 2012). This is realised through a sequence of rotations that account for the precession and nutation involved in Earth rotation, as well as polar motion (Schuh and Behrend, 2012). The complete set of these parameters are the five EOPs (two precession/nutation parameters, two polar motion, and one for universal time). These are the Earth orientation parameters which, somewhat obviously, define the orientation of the Earth. A precise determination of these is important for a range of applications and is a priority for global geodesy. VLBI is the only space-geodetic technique to be able to determine all five EOPs due to its unique ability to measure the universal time (usually given as UT1–UTC).

There are a variety of more specific applications for the data collected in geodetic VLBI sessions. Tropospheric parameters, such as the VLBI zenith wet delays, are particularly important for climatology as they contain precipitable water vapour information for the region of the troposphere above each station, for as long as the station has been operating (Böhm et al., 2003). Ionospheric models (Hobiger et al., 2006) as well as the frequency dependent Love and Shida numbers for solid Earth tides, which characterize the Earth’s response to tidal forces (Krásná et al., 2013) are also supported by geodetic VLBI results. In addition to these more terrestrial applications, VLBI sessions have also been used to observe the gravitational deflection of radio waves according to general

relativity (Schuh and Behrend, 2012).

In this project, however, we primarily focus on considering the precision of EOPs and station coordinate results made possible with current and future geodetic VLBI experimentation.

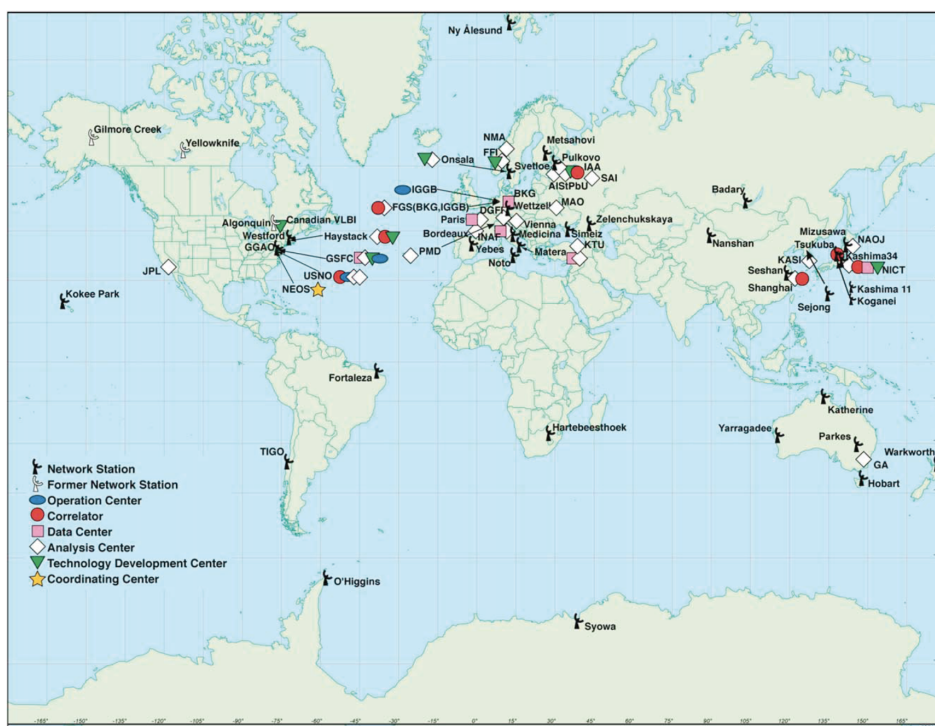
2.1.3 A Governing Body: IVS

The contributions to global geodetic products have become increasingly coordinated and therefore, increasingly comprehensive and precise, since the end of the last century. This is due to the advent of a clearly defined governing body for VLBI stations and networks worldwide.

The IVS became an approved service of the International Association of Geodesy (IAG) in March 1999 and has been a member of the International Astronomical Union (IAU) since 2000 (Nothnagel and Behrend, 2016). The IVS itself is a collaboration of organisations which work together to operate or support VLBI components for geodetic, geophysical and astrometric research, rather than an independent body (Nothnagel et al., 2016a). According to the 2011-2015 IVS Summary of Nothnagel and Behrend (2016), its primary goals are to promote research and development in all aspects of the geodetic and astrometric VLBI technique; interact with the users of VLBI products; and integrate VLBI into a global Earth observing system.

By nature, the IVS does not have individual assets, so it must rely on its member organisations, operating on a best-efforts basis, to achieve these goals (Nothnagel et al., 2016a). In recent years however, it has supported a range of projects for developing and maintaining reliable state-of-the-art VLBI systems worldwide, through the general support and goodwill of the geodetic community. The IVS allows for structured coordination of the global observing program, development and analysis (Nothnagel et al., 2016a).

An IVS Coordinating Centre and multiple IVS Operations Centres are co-located with VLBI stations around the world. Figure 2.3 is a depiction of the IVS’s global infrastructure with the nature of each individual component



identifiable from the symbol key.

Through the support of these centres, the IVS is able to organise a range of observation programmes, allocate scheduling, correlation and first-stage analysis resources while also taking into account the participation capabilities of each of the global VLBI stations in the network (Nothnagel et al., 2016a). Thus, a strategic, integrated, and global effort for the determination of highly precise EOPs, as well as the development of the CRF and TRF is made increasingly efficient and effective through the infrastructure of the IVS.

2.2 Scheduling Theory and VieVS

Coordination of resources is necessary for the success of any scientific program. For geodetic VLBI, this is predominantly seen in the form of effective scheduling. The experiment schedule has a significant impact on the optimisation of

global resources and the quality of experimental results. Most obviously, with the large number of institutions globally that are required to work in tandem to achieve the range of operational goals, management through scheduling is imperative. Less intuitive but perhaps more importantly, each schedule will also affect individual geodetic sessions and their corresponding output. As such, this idea of effective scheduling and the scheduling process itself, is often subjected to much consideration and analysis by the global geodetic community. The following section is simply a brief outline of the current scheduling practices for geodesy on which the analysis in this project is based.

2.2.1 Scheduling for Operation

To coordinate the growing network of global, geodetically capable stations, the IVS manages a predefined observing program through annual master schedules. These consider the main scientific aims of the community, as well as station availabilities in an attempt to maximise the capability of the entire IVS network. Most of the sessions span a period of 24 hours, due to the dependence of geodetic results on diurnal effects and nutation over the Earth’s rotation. This is with the exception of the daily 1 hour sessions for UT1–UTC. Each session will usually have a primary scientific focus but, with effective scheduling, also be able to produce all types of possible geodetic and astrometric results (Nothnagel et al., 2016a).

As mentioned previously (see Section 2.1.2), the precise determination of EOPs is an important scientific and operational goal for geodetic VLBI. Maintaining the TRF and CRF is also a priority. These are supported by regular research and development (R&D) sessions and a number of continuous observing campaigns. There is a standard procedure and order of priority for the consideration of each of these goals in the planning of the IVS master schedule. This streamlines the process of scheduling, which presently requires considerable time and human resources.

A standard week of observations is presented in Figure 2.4. EOP dedicated

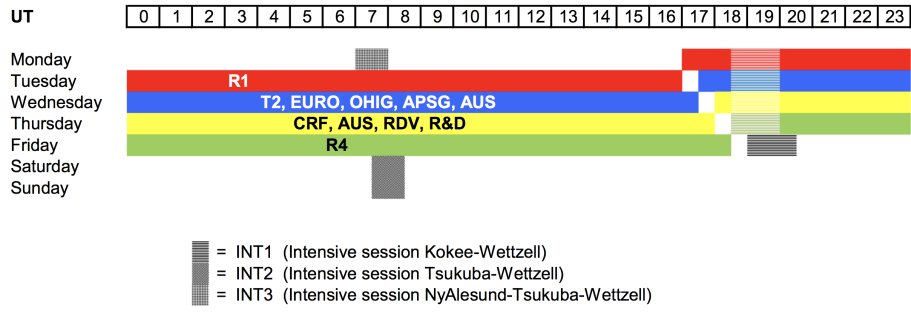


Figure 2.4: A typical IVS observing week which consists of three or four 24h sessions and at least one 1h Intensive session every day. To optimize data transport and to avoid weekend 24 hour sessions, the observing week commences on Monday at 17:00UT with an R1. Following each 24 hour session, there is a 30-min break before the subsequent session starts. The concluding R4 session finishes on Friday at 18:30UT. The Intensive sessions are observed by a small number of stations, either in parallel to the 24h sessions or during the weekend time (Nothnagel et al., 2016a).

observing sessions occur bi-weekly on Mondays and Thursdays involving approximately 8 global stations, depending on availability. These are the IVS R1 and R4 experiments which prioritise a rapid turn around on results which are made available, usually, no later than 15 days after each session. UT1–UTC is monitored with the 1 hour long Intensive sessions which are run daily, usually on a single baseline. The TRF and CRF are prioritised in sessions which occur bi-monthly, as well as some regional network sessions. The CRF is predominantly monitored by the Very Long Baseline Array (VLBA) and up to eight geodetic stations (RDV). Sources in the southern sky, infrequently observed historically, are also a focus of many astrometric sessions for the CRF. The TRF sessions require a contribution from a large global network with approximately 14-18 stations and it has been determined that the whole network must observe for at least two full sessions per year (Nothnagel et al., 2016a).

In addition to these standard sessions, R&D for the improvement of the entire global network is prioritised in a dedicated session once a month. This may be to study instrumental effects, EOP network biases or to test new developments in technology or practice. The other unusual observing session type favoured by the IVS master schedule is the triennial, continuous observing

periods which are specified to be observation sessions of 2 weeks in duration. These ‘CONT’ experiments are designed to maximise the amount of sustained, high quality observations; produce a very dense time series; and demonstrate the best results geodetic VLBI is capable of producing at the time. However, considering that the average time per week usually committed to VLBI sessions is approximately 3.5 days, the increase to continuous observing is significant (Nothnagel et al., 2016a). This is why such sessions currently are only scheduled on a triennial basis. As discussed in Section 2.3, however, they represent the future goals of geodetic VLBI.

Currently, there are approximately 180 geodetic sessions scheduled per year on the IVS master schedule (Nothnagel et al., 2016a). These are all capable of producing notable results for determining EOPs, the TRF, CRF and constantly improving the technological capabilities of geodetic VLBI. Scheduling well in advance allows the IVS to manage the goals and priorities of the entire global network as well as to manage the many hours and human resources required to coordinate such experiments. It is a system that has worked for many years of good geodetic results. However, as a system, it is very susceptible to last-minute changes, operator errors or equipment failure, which is exacerbated by the effective operational isolation of each individual site during a session (Lovell et al., 2016). Hence, there are still a number of areas for improvement in the scheduling for future geodetic operations.

2.2.2 Scheduling Priorities for Geodetic VLBI

The theoretical concept behind scheduling for geodetic VLBI is simple: determine the sources to be observed by particular telescopes at particular times over the duration of the experiment. As with most simple ideas, however, in practice this is not so straightforward. Scheduling is a complex optimisation problem where a scheduler must find a balance between the best results theoretically achievable, the technological capabilities of the network and the influences of the natural environment. For geodesy, this is usually completed

with specifically designed software and an operator defined set of scheduling priorities.

Within the geodetic community there exists a range of different optimisation strategies, considering a variety of scheduling parameters to varying degrees in the scheduling process. Usually, this is dominated by the station-based approach in which the sky coverage is optimised over a certain period with weighting factors applied on other parameters (e.g. Schartner, 2017).

Simply put, the sky coverage is a parameter which describes the number of sources in different areas of the sky or how well the sky is covered by observations. The reason this is particularly important for geodetic VLBI is due to the troposphere. Errors brought about by unpredictable fluctuations in the troposphere are considered to have the largest detrimental effect on geodetic results. These cannot be prevented but their effect is lessened by increasing the number of observations in as many different directions and elevations as possible for each station (Plank et al., 2017).

As a proxy, sky coverage can be represented as the number of scans per hour for an individual station (Plank et al., 2017). In geodetic VLBI, a scan is defined to be the case where a particular source is observed by more than one station in the network. Each baseline observing this particular source during the scan contributes one observation. As such, we can define the number of observations for any given scan as the number of possible baselines to observe that source:

$$n_{\text{baselines}} = n_{\text{stations}} \times \frac{(n_{\text{stations}} - 1)}{2} \quad (2.6)$$

On the small AuScope network, an even simpler rule of thumb can be considered for geodetic purposes: ‘the more observations, the better’ (Plank et al., 2017).

There are two obvious methods to maximise the number of observations. Considering Equation 2.6, it is possible to see that increasing the number of

stations will result in an increased number of observations. However, this is not always possible due to limited joint visibility between stations and the finite number of geodetic VLBI antennas worldwide. Hence, it is often more effective to consider maximising the number of scans completed within an experiment.

This is achievable by minimising the time required for each scan and the time required to slew to new sources. The slewing rate is a product of the individual antennas in the network and cannot be manipulated but must be accounted for in the schedule. The time needed for each scan is reliant on the relationship between the required SNR for a reliable fringe detection, which is governed by the brightness of the source to be observed (i.e. flux density F) and the sensitivities of the two receiving antennas (in system equivalent flux density SEFD), and the amount of data that is recorded per time unit per band (the data rate). This is presented in Equation 2.7 for up to 2 bit sampling:

$$t_{scan} \propto \left(\frac{SNR}{F} \right)^2 \times \frac{SEFD_1 \times SEFD_2}{data\ rate} \quad (2.7)$$

Hence, it is possible to see that scheduling based on optimising just the sky coverage is already a complex problem which depends on a range of embedded optimisation problems. However, simply increasing the number of observations is only a first-order method for scheduling effective geodetic experiments. There is much further depth to this process which is not discussed here. Figure 2.5 shows a representation of these complexities in a simple flowchart. It is based on the presentation of Schartner (2017) for developments in scheduling with the Vienna VLBI Software (discussed further in Section 2.2.3) which allows for significant flexibility in scheduling priorities.

Work to improve what we know and understand about scheduling is ongoing. This is one reason that a range of scheduling processes and corresponding software continues to be developed. It is important to consider the scheduling priorities and parameters which will generate the best possible schedule for the

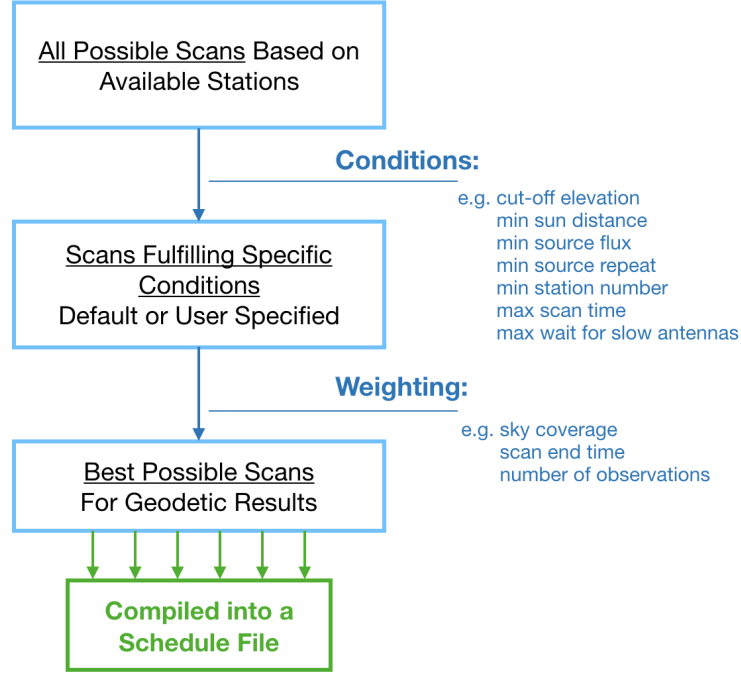


Figure 2.5: A representation of the complexity of the optimisation processes involved with scheduling, based on the developments in the Vienna VLBI Software as presented by Schartner (2017)

desired geodetic results.

2.2.3 Software: VieVS

The Vienna VLBI Software (VieVS) was used to generate the schedules for this study. This is a common MATLAB-based scheduling and analysis tool developed at the Institute of Geodesy and Geophysics in Vienna for increased capability in line with the present and future requirements of geodetic VLBI (Böhm et al., 2009). Such requirements are discussed further in Section 2.3.

The VieVS system is designed to be consistent with the International Earth Rotation and Reference Systems Service (IERS) Conventions and IVS standards in order to generate results which are comparable to other space-geodetic techniques, such as Global Navigation Satellite Systems (GNSS) or Satellite Laser Ranging (SLR). It is based in the MATLAB computing environment.

VieVS also allows for more programming and usage opportunities for the range of different personnel involved in geodetic VLBI, even those who may not necessarily be particularly proficient in source-based coding. This is because it takes advantage of many of MATLAB's built-in tools and functions to develop a significantly more user-friendly interface than a number of its contemporaries and predecessors. The parameterisation with piece-wise linear offsets at integer hours in the least-squares adjustment also provides a high level of flexibility and comparability (Böhm et al., 2009).

VieVS is capable of scheduling, simulating and analysing a range of different geodetic experiments and the corresponding results. Common sources of error and a variety of other parameters can be individually considered. In recent years, significant work has been put in to an effective simulation of wet troposphere delay, station clock, and measurement errors. These are the three main stochastic error sources in VLBI and all are considerable within VieVS (Pany et al., 2010). As such, it is possible to use VieVS as a tool to both analyse these sources of error individually or to modulate other simulated results with their varying effects, improving the simulations' correlation with observable results. The system also lends itself to producing Monte Carlo simulations of group delay observables, such as those considered in preparation for VGOS (e.g. Pany et al., 2010; Nilsson et al., 2007).

Figure 2.6 shows an example of the VieVS interface. It is possible to clearly see the range of options easily accessible for identification and modification. The VieVS platform is being used in a range of dedicated research and development projects, as well as in the corresponding prototyping, system studies and Monte Carlo simulations worldwide. The MATLAB-based interface provides an efficient method to study, plan, and manage future observing scenarios, antenna specifications, station networks, and analysis strategies (Pany et al., 2010). The results discussed in following chapters, are one such example of this functionality.

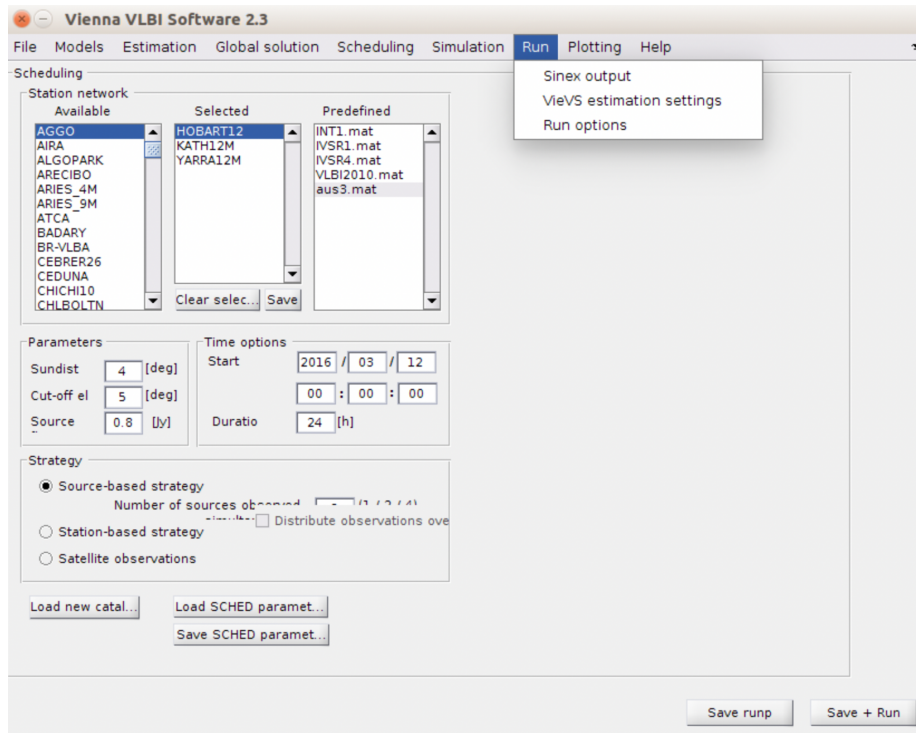


Figure 2.6: An example of the VieVS interface. The General Scheduling parameters window is open with the Run tab displayed. This is Version 2.3, although this has since been superseded by Version 3.0.

2.3 Next-Generation Aims: VGOS

In September 2005, a working group of the IVS completed a review of the current VLBI systems and processes to then outline a set of recommendations for the next-generation of operation, covering a range of areas from antenna specifications to geodetic analysis capabilities. These recommendations became known as the goals of VLBI2010: 1mm position accuracy on a global scale; continuous measurement for a dense EOP and station coordinate time series; and, turnaround times of less than 24 hours for initial geodetic results (Petrachenko et al., 2009). Over the intervening years, a more specific plan for implementing this next-generation of geodetic observation has been developed. This became what we now refer to as VGOS following the 7th General Meeting of the IVS. The members of the IVS are currently in the process of transitioning to this new level of operation (Nothnagel and Behrend, 2016).

The first successful session using the proposed VGOS observing mode was observed on 13 May 2013 with the GGAO12M [Gs](Goddard Space Flight Centre, MD USA) - WESTFORD [Wf] (Haystack, MA USA) baseline. Over 99% of the scans yielded good correlation (Nothnagel and Behrend, 2016) and as such, it was determined to be a success.

2.3.1 VGOS and its Intended Outcomes

The VGOS network is to be a global network of antennas with fast drive speeds (up to 12 deg/s), high capacity data acquisition systems (up to 32 Gbps) and new broadband observation modes (2-14 GHz). It will form the VLBI component of the Global Geodetic Observing System (GGOS) and will make a significant difference to the standard of observations possible with geodetic VLBI at the present time. The global VGOS network will form a system that is optimised for Earth orientation determination and maintenance of the TRF. Hase et al. (2012) envisioned VGOS operation to be possible by 2018 with the legacy S/X mode also maintained in parallel for data continuity, astrometry, and space applications.

The transition to full VGOS operation is predicted to take a number of years, however, as technology, practices and station sites develop. Petrachenko et al. (2009) indicate that, for VGOS capability, a network of at least 16 globally distributed stations should be operating at all times for EOP determination, plus a number of additional stations to maintain the CRF and TRF. In order to reach this 24/7 capability, stations are planned to be upgraded or created for VGOS capability annually until the goal is met (Hase et al., 2012). It will also be important for at least a subset of these VGOS stations to be capable of providing the required fast delivery of initial data to produce IVS products within the 24 hours turnaround time.

The number of stations in the Southern Hemisphere must also be increased (Petrachenko et al., 2009). Figure 2.7 is a depiction of the proposed global VGOS network and each station's global coverage and properties, such as an-

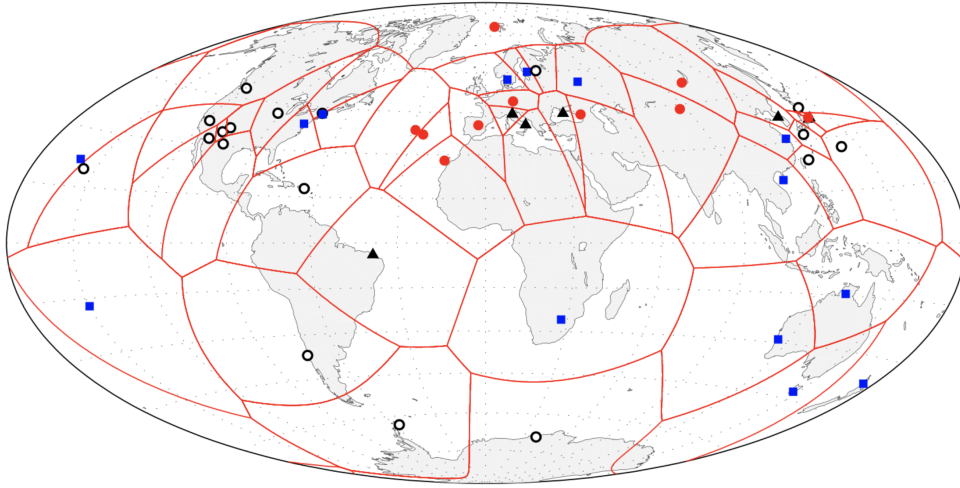


Figure 2.7: *Predicted total IVS network for 2018 consisting of new VGOS stations, upgraded stations, and legacy S/X network stations. The Voronoi diagram is based on all network stations. Red circles indicate very fast moving telescopes and blue squares, fast moving telescopes. The upgraded legacy telescopes are marked with black triangles and S/X sites without major upgrades with hollow circles (Hase et al., 2012).*

tenna speed and receiver type. The station coverage is represented by a Voronoi diagram showing the lines of maximum distance to the next VGOS station. As such, the size of the blocks in a specific region indicates the density of the network in that region. It is possible to identify that the Southern Hemisphere is still significantly more sparsely populated than northern latitudes and that the entire distribution is non-homogeneous (Hase et al., 2012). Hence, it is an ongoing goal to increase the number of stations in the South (Petrachenko et al., 2009) and in the interim to increase the number of observations by existing stations (Plank et al., 2017).

The number of stations in the proposed VGOS network is large, significantly greater than the recommended number of approximately 16 continuously operating antennas. This is so that each and every station in the network is not committed to operating 24/7. Instead, the load of continuous observation is to be spread throughout the total number of IVS stations available at any given time to ensure continuous availability of EOP results (Nothnagel et al., 2016a). This is another reason why it would be beneficial to increase

the number of Southern Hemisphere antennas since the commitment load on these stations is higher than their northern counterparts. This is due to the obvious visibility reasons: only a small number of stations can assist with observing southern hemisphere sources, so the commitment weight of those observations must be split among the a severely limited number of stations with joint visibility at any time. It is nevertheless important to manage the commitment of continuous observing since this will enable polar motion, nutation and UT1–UTC to be monitored continuously. This is a factor which is predicted to bring about the improvement in precision required to make the IVS a strong contender as the primary source for polar motion information (Nothnagel et al., 2016a).

The VGOS observing mode is not only designed to generate more precise EOP contributions but also to improve the accuracy of defining station positions. Petrachenko et al. (2009) assert that, while the atmosphere is the dominant source of error in station coordinates, shortening the source-switching interval is almost proportional to the corresponding improvement in station position accuracy. As a result, VGOS aims to decrease both the on-source time and the time required to slew between sources. To achieve this while still being capable of taking a precise delay measurement is somewhat complex.

Petrachenko et al. (2009) recommend either a single very fast 12m antenna with a slew rate of approximately 12deg/s in azimuth, or a pair of fast 12m antennas, each with the moderate slew rate of approximately 5deg/s in azimuth, in order to account for the time required to slew between sources. To limit the time required on-source to measure a precise delay, even with modest SNR, a new mode of observing has been developed. This is called the broadband delay and it relies on several widely spaced frequency bands spanning the entire frequency range from 2 to 14 GHz to unambiguously resolve the interferometric phase (Petrachenko et al., 2009) discussed previously. This imposes a limit on the data rate since, according to Petrachenko et al. (2009), to detect sufficient high-quality radio sources in this manner will require a total instantaneous

data rate as high as 32 Gbps and a sustained data storage or transmission rate as high as 8 Gbps.

VGOS is specifically designed to improve the main output of geodetic VLBI in terms of EOPs and station coordinates in particular, but it also seeks to promote continued development in general, through limiting the causes of existing errors. For example, systematic errors such as electronic biases, antenna deformation and source structure are all accounted for in the aims and outcomes of VGOS operations (Petrachenko et al., 2009).

2.3.2 Primary Areas of Concern

The goals of VGOS for the next era of geodetic VLBI observations are promising for significant development in the field. However, they are incredibly ambitious and, therefore, are associated with a number of major hurdles to overcome (Nothnagel et al., 2016b). The two main concerns for the successful implementation of VGOS are the significant increase in data volume to be managed by the network and the number of resources required to increase the number of observations. Petrachenko et al. (2009) also identified radio frequency interference (RFI) as an increasing concern, although they note that VLBI is comparatively insensitive to RFI over other sources of error and consequently VGOS has been designed for the maximum possible resilience so that this does not factor as an major concern in the future.

The data volume issue is not so simply solved. Due to the smaller size of VGOS antennas and the corresponding increase in total number of observations per session, even if the number of operations were constrained to the current number at VGOS capability, there would be a large increase in data volume (Petrachenko et al., 2009). Currently, data volumes are approximately 2-6 TB/day but VGOS goals would require 16 TB/day or more per station (Petrachenko et al., 2014). Bearing in mind the goal of a turnaround time of less than 24 hours to initial geodetic results, this poses a significant problem for the transition to full VGOS.

With current technological capabilities it will not be possible to manage this goal (Haas et al., 2017). Some IVS stations, such as Hobart, have high data movement capabilities through their access to optical fibre connections with capacities of 10 Gbps or more, but the data rates required for VGOS are much faster than this, especially at the correlators. However, these correlators themselves do not yet have even the 10 Gbps capability (Haas et al., 2017). In order to manage the overwhelming data rates in real-time, significant technological advancement must be made in the area of data transfer and upgrades to many existing connections must be made globally.

Aside from data volume, increased operation times generates a number of other concerns for many stations across the globe. This can be seen particularly in terms of the increased cost and resources required. For many stations, increasing from the standard 2-3 sessions/week to even close to 24/7 operation is currently impossible. The global transition is limited by the resources of its smallest contributors. As such, the need to introduce automation and remote control to the network has become a development priority.

Automation in both station operation and analysis will reduce the cost of increased operations (Petrachenko et al., 2009). Currently, work is ongoing to make all processes involved in geodetic observation such as schedule generation, station operation, correlation, fringe processing, and analysis, as automated as possible (Nothnagel and Behrend, 2016). The dynamic observing of Lovell et al. (2017), discussed in Chapter 4, is one example of automating these processes.

Remote control is also identified as important to the successful implementation of VGOS (Nothnagel and Behrend, 2016). This aligns well with the initial ideas for the practical application of VGOS where observing stations will be monitored centrally to ensure compatible operating modes, update schedules as required, and notify onsite staff when problems occur (Petrachenko et al., 2009). However, complete remote operation is not feasible for many sites for a variety of reasons (Lovell et al., 2016). Hence, there is still much work to

be done in the geodetic VLBI community to improve the efficiency of resource management, potentially through automation, in order to cope with the operational increase which will come with full VGOS.

2.4 The AuScope VLBI Network

The AuScope VLBI network referred to in following chapters is the name given to the relatively new geodetic VLBI array which is part of the Australian AuScope project (Lovell et al., 2013). It is defined to comprise of the three identical 12m radio telescopes situated across Australia at Hobart [Hb] (Tasmania), Katherine [Ke] (Northern Territory) and Yarragadee [Yg] (Western Australia).

This section will outline the technical specifications, operations and goals of the network in some detail. These are important as the AuScope VLBI network forms the basis for much of this study.

2.4.1 Technical Details

The geographical location of each of the AuScope 12m antennas can be seen presented in Figure 2.8. A line between each station indicates the three baselines and their lengths are also specified. The longest of the Australian baselines is between Hobart and Katherine (Hb-Ke) at 3234km, although compared to most global baselines this is still comparatively short. The shortest Australian baseline is between Katherine and Yarragadee (Ke-Yg) at 2360km and the baseline between Hobart and Yarragadee (Hb-Yg) forms the last side of the network at 3211km.

The VLBI antennas of the AuScope network are positioned to maximise the area covered by the network on the Australian continent while minimising the disruption from the large population density regions on the East Coast. In addition, they are intentionally located alongside other space-geodetic facilities such as GNSS (see Figure 2.8) and gravity infrastructure. The Yarragadee site also has Satellite Laser Ranging (SLR) and Doppler Orbitography and

Radiopositioning Integrated by Satellite (DORIS) facilities operating on location. In these ways, the geographical location of the AuScope VLBI array was strategically selected to optimise the potential contributions of such a network to the CRF and TRF in the Southern Hemisphere (Lovell et al., 2013).

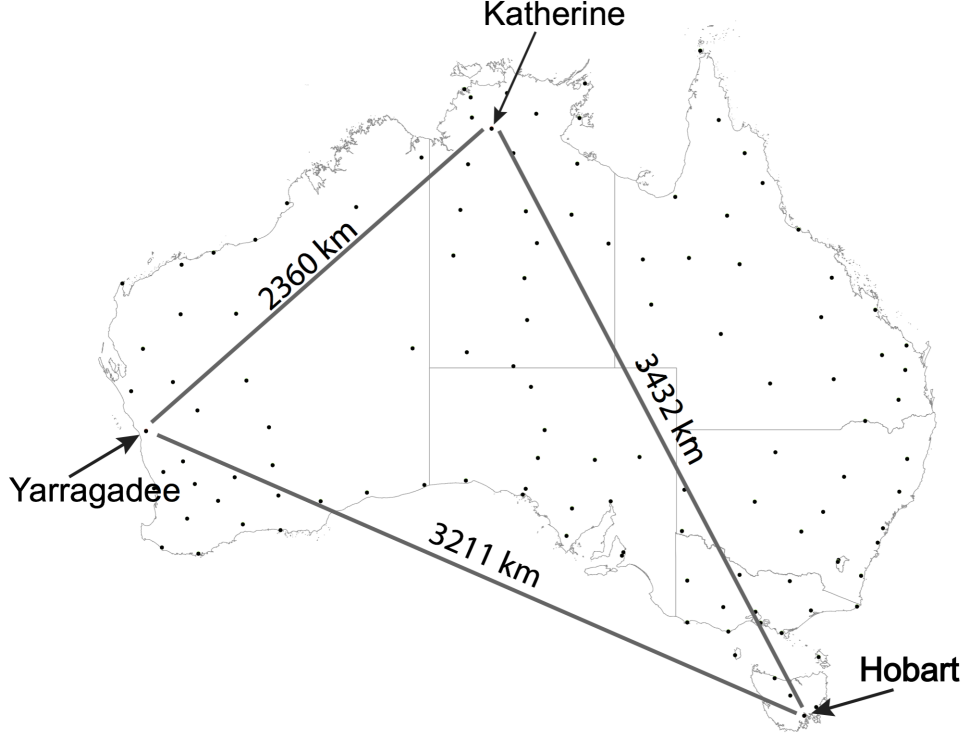


Figure 2.8: *The geographical location of new AuScope VLBI array and GNSS infrastructure. The 12 m telescopes are labelled by name and connected by their respective baselines. Filled dots indicate GNSS sites (Lovell et al., 2013).*

The AuScope network operates as part of the IVS observing program and with smaller regional collaborations, but it is also fully capable of independently planning, scheduling, observing, correlating, and analysing its own VLBI experiments. The entire network can be coordinated and controlled remotely by a single operator from a dedicated operations room at the University of Tasmania, approximately 20km away from the Hobart station. In fact, this is common practice for operations since one of the main goals for the AuScope network is increased remote capability. The array was specifically designed to manage remote operation. Through the use of a range of redun-

dant and externally resettable systems, it is ensured a high resilience to onsite failures or connection losses (Plank et al., 2017).

The observations are able to be coordinated by a single operator in Hobart through the running of the eRemoteControl software of Neidhardt et al. (2010) on the control room computer for each antenna. Site-specific parameters, such as recording temperatures, motor currents, and wind speeds are monitored in a similar manner by the openMoniCA software of the Australian Telescope National Facility (ATNF). A server system is used to access the local field system machines, DBBCs, Mark5 racks, and drive PCs at each station. A variety of useful operator developed scripts and procedures then enable efficient operation and monitoring of the multiple antennas. For example, there is an automated data checking procedure which performs an autocorrelation for each scan and graphically displays the result; a program to run fringe checks on a strong calibrator with the AuScope antennas through simple command line prompts; a live DBBC formatter time monitoring program to identify a range of operational issues; and many other useful facilities (Plank et al., 2017).

As convenient and reliable as remotely operable control systems may be, the largest limiting factor to remote operation in Australia is connection capability. The Hobart site is connected to the University of Tasmania through a 10 Gbps connection and then to the Australian mainland at the same data rate. However, the site at Yarragadee is only connected through an ADSL internet line and Katherine shares access to a 10 Mbps connection through the nearby Charles Darwin University (Plank et al., 2017). In the case of these two stations, connectivity is a major concern to remote operations. With experience, practices have been implemented in the AuScope observing routine to ensure resilience to these kinds of complications. Although, modules must still be physically shipped to Hobart for transfer on the stronger connection (Plank et al., 2017).

The design of the array and antennas themselves was directed to match the VGOS requirements as closely as possible with capabilities at the time but

also to allow for the opportunity to upgrade in the future (Lovell et al., 2013). A representation of the 12m telescopes is presented in Figure 2.9 with some of the major parts identified.

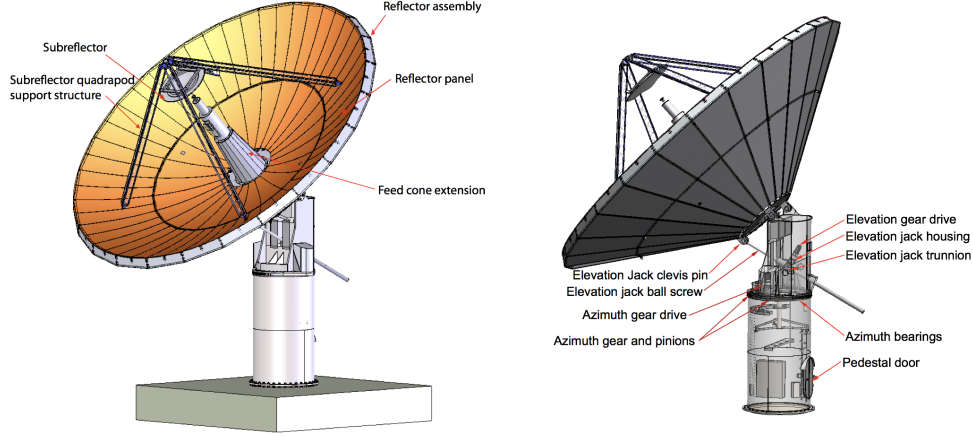


Figure 2.9: *Representations of the 12m antennas used in the AuScope VLBI array and their main components (Lovell et al., 2013).*

The antennas are each mounted on a pedestal with reflectors of an identical 12m cassegrain shape and it is noted that a number of the following design specifications for the AuScope antennas are unique in this size range (Lovell et al., 2013). Each is equipped with a legacy S/X receiver giving them an operating frequency range of 2.2-2.4 GHz at S-Band and 8.1-9.1 GHz at X-Band (Lovell et al., 2013). Since they are only 12m in diameter compared to the usual $\geq 20\text{m}$, the size of these antennas makes them less sensitive than other legacy equipped stations in the IVS network (Plank et al., 2017). However, the AuScope design specifications prioritised drive speed and as such, each antenna can slew at up to 5 deg/s in azimuth and 1.5 deg/s in elevation (Lovell et al., 2013). This makes these fast antennas capable of switching between sources much more quickly and efficiently than other legacy stations but they are yet to achieve the slew speeds of the ideal very fast VGOS antennas which aim for a standard of 12deg/s in azimuth and 4deg/s in elevation for an individual station (Plank et al., 2017).

The fast drive capabilities of the AuScope 12m antennas are also supported

by state of the art back-ends and recording systems (Lovell et al., 2013). A DBBC-2 system is used as the main data acquisition system for each antenna with Mark5B+ units for recording (Plank et al., 2017). Here, again the AuScope network has introduced redundancy for improved resilience to last-minute failures and improved remote operational capability. Each site is equipped with two Mark5B+ recorders and, on the whole, the network owns and operates more than 100 Mark5 modules with capacities of up to 32 TB each (Plank et al., 2017).

2.4.2 Formation

The AuScope VLBI array was able to be developed and constructed thanks to funding from the Department of Innovation, Industry, Science and Research as a part of the National Cooperative Research Infrastructure Strategy (NCRIS) (NCRIS, 2006). The VLBI array forms only one part of the diverse framework of infrastructure supported through the AuScope project, which attempts to align the geological, geochemical, geophysical, and geospatial research fields in Australia (AuScope, 2012).

The array is coordinated through the Hobart site, as this was already an important IVS station for almost 20 years prior to AuScope. The Hobart 12m telescope, discussed in the previous section, was built at the Mt. Pleasant Observatory in addition the existing 26m telescope at that site. The Hobart 26m antenna [Ho] has been an member of the IVS network (and its various predecessor cooperatives) for more than 20 years and is one of the only Southern Hemisphere sites to be able to work all year round with rapid data transfer to the correlation centres in North America and Europe (Lovell et al., 2013).

In fact, the Hobart 26m was the only Australian telescope to contribute regularly to geodetic and astrometric experiments between 1989 and 2011, although the Parks 64m and the DSS45 34m antennas did contribute on occasion (Plank et al., 2017). As such, the Hobart telescope was essentially geographically isolated and correspondingly, its overall geodetic performance was found

to be poor when compared to similar Northern Hemisphere antennas (e.g. Titov, 2007). Southern hemisphere observations are also particularly important for VLBI experiments as sources with $\text{Dec} \leq -40^\circ$ are not visible to most Northern Hemisphere arrays. Hence, to expand the ability of the IVS to monitor the southern-most ICRF sources as well as support the geodetic applications of the Hobart 26m antenna, increasing the number of Southern Hemisphere telescopes was determined to be a priority (Lovell et al., 2013).

Consequently, five of the nine antennas at southern latitudes were built after the year 2010 (Plank et al., 2017) and one-third of these nine southern telescopes is made up by the AuScope network's three 12m antennas. The effect of adding these telescopes can be seen in Figure 2.10 which depicts the contributions of global IVS stations to geodetic measurement between the years 2010-2015. Here, the blue dots indicate the position of stations on the globe and the size of the dots is proportional to the number of recorded observations in that year. It is clear to see that, even in this 5 year period, there was a significant increase in the number of Southern Hemisphere observations.

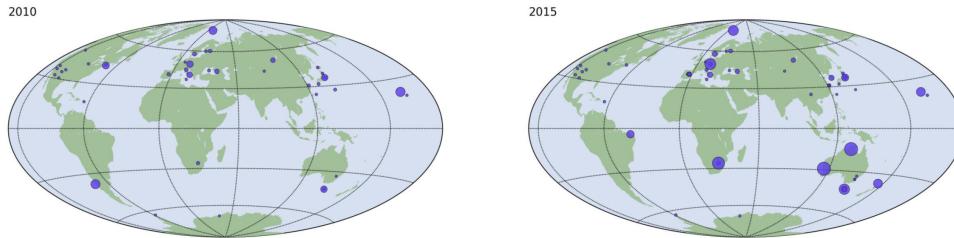


Figure 2.10: *Two depictions of station geodetic VLBI activity for the years 2010 and 2015. The blue dots indicate the position of stations on the globe. The size of the dots is proportional to the number of recorded observations in that year. Even in this 5 year period, there is significant increase in the number of Southern Hemisphere observations (Lovell et al., 2017).*

Unsurprisingly, the 12m at Hobart was the first of the three new telescopes to become operational. Construction was completed in 2009 and the antenna was officially accepted into the IVS at the General Meeting on 9 February 2010. The first successful observation in which the Hobart 12m participated

in an IVS session was in October 2010 after a period of commissioning, testing and debugging. All three AuScope antennas were completed and able to successfully observe in IVS sessions by June 2011 (Lovell et al., 2013).

Since then, the AuScope network has been working toward the goal of increasing the density of geodetic observations in the Southern Hemisphere. Its increasing contribution to the CRF significantly improves the TRF through the detection and correction of systematic errors. It is also useful for an improved measurement of the Australian tectonic plate’s intra-plate deformation (Lovell et al., 2013). The AuScope array as an individual network, in sessions with the IVS network or as part of the regional sessions, is also an important tool for the determination of source positions, absolute station coordinates to millimetre accuracy, un-modelled station movements and all five EOPs (Plank et al., 2017).

2.4.3 Present Operations: AUSTRAL

Most of the AuScope network’s present geodetic operations involve some kind of collaborative work with similar IVS stations around the world, predominantly to define and monitor the geodetic reference frame and thereby improve the geophysical interpretation of space geodetic data. Most of the correlations for these types of sessions are conducted by IVS correlators in Bonn (Germany), Washington or Haystack (USA) (Lovell et al., 2013).

Outside of the regular IVS R1 and R4 experiments, a large portion of observation time on the array has been dedicated to the AUSTRAL observing program. This program, which commenced in 2011, relies on a variable Southern Hemisphere array of similar telescopes including, but not limited to, the three 12m AuScope antennas, Warkworth 12m [Ww] (New Zealand) and Hartebeesthoek [Ht] 15m (South Africa). It was essentially created to take advantage of the AuScope network’s full operational capabilities and AUSTRAL sessions are mostly managed entirely by the control centre in Hobart (Plank et al., 2017).

Approximately 150 successful AUSTRAL sessions were observed between 2011 and 2016 and the program is still ongoing. More than half of these sessions (81) involved the five-station network (Hb Ht Ke Ww Yg); a total of four stations observed in 42 sessions (Hb Ke Yg and either Ww or Ht); and there were 22 sessions with only the three AuScope antennas (Hb Ke Yg). The remaining sessions had good data from only 2 stations or further additional global stations were included. The session types ranged from the common 24 hour single sessions to 48 hour weekend sessions and long 15 day continuous campaigns (Plank et al., 2017). The scientific objectives were also often varied such as obtaining accurate geodetic results, a dense time series, or sessions with astronomical purposes.

From the full range of the AUSTRAL sessions a median 88% of scheduled observations are seen to be successfully correlated (Plank et al., 2017). This is considered as a measure of experimental success. It is also promising to see most of the missed scans are due to SNR, wind stows or other small technical issues. The operations of the five stations consistently involved in the AUSTRAL sessions, including their standard IVS contributions, between 2011 and 2015, produced the most dense geodetic VLBI time series ever achieved (Plank et al., 2017). It is possible to see that the AuScope network and the AUSTRAL sessions are well achieving the goal of increasing the number of good observations at southern latitudes.

In addition, the geodetic results obtained from these sessions are seen to be comparable with those produced in standard IVS sessions. The absolute station position coordinates found were determined to be consistent with similar IVS values and baseline repeatabilities are generally found to be better for the AUSTRAL baselines. However, it seems that the weakness of the AUSTRAL network on the whole, is in determining polar motion. On the other hand, the strength of the sessions is to estimate accurate source positions between declination -20 deg and -50 deg. That is, sources in the area immediately above the network. The findings from the AUSTRAL's 'astro' sessions were

also promising for the field of astrometry (Plank et al., 2017).

The AUSTRAL experiments, along with some observing programs with the Asia-Oceania VLBI (AOV) group (Kurihara et al., 2014), have also proven that many stations are willing and able to contribute to collaborations at short-notice, in addition to their yearly commitment to the IVS. This is particularly evident for the AUSTRAL sessions with ad-hoc scientific targets, such as AUA011, AUA012, AUA020, AUA029 and AUG020, where stations from Australia, New Zealand, South Africa, China, Japan, South Korea, Russia, Italy, Sweden, and Spain volunteered observation time (Iles et al., 2017). This kind of collaboration shows the development of institutional priorities and the associated results that can be achieved as the global geodetic community transitions the next era of observation.

2.4.4 Future Goals

As discussed in Section 2.3, the IVS is currently undergoing a period of large-scale development. This will involve increasing the total number of observations through improving the standard of antenna drive speeds and shortening the time required on each source by using higher data rates or improved sensitivity. In these areas, the AuScope network is well poised to make the transition to VGOS as it was designed for such capabilities, see Section 2.4.1. One of the more difficult features of an antenna to change significantly after the fact is the required slewing time. As such, in the transition to VGOS many observatories are choosing to build smaller, faster antennas like the AuScope 12m antennas. As far as sensitivity, currently, the AuScope network is equipped with legacy S/X receivers but work has already commenced to begin the transition to broadband VGOS receivers and soon the network will be capable of observing in full VGOS mode (Plank et al., 2017).

However, the most ambitious goal of the VGOS observing plan is not the receivers or slew speeds but continuous 24/7 operation. To make this a reality, the entire global geodetic community must adapt operational requirements.

Human resources and data management, for example, would be overwhelmed by continuous observation in their present state. Increasing automation over a range of common operational processes has been proposed as a viable way to achieve this (e.g. Plank et al., 2017). Again, the AuScope network is in an advantageous position due to its capacity to remotely manage the entire network from a single control room. This allows for more observations with less impact on cost and human resources, as well as greater flexibility in the scheduling of sessions with a range of different priorities, including technological development in this way (Plank et al., 2017).

Development in technology and observational precision is a major priority for the AuScope network moving into the near future. This includes an implementation of elevation dependent SEFD values in the scheduler for further optimisation of the scan length and a new observing mode capable of data rates up to 2 Gbps using the current hardware (Plank et al., 2017). There is also an ongoing focus on improving the reliability and physical performance of each station since this is still a relatively new and developing network. Increased automation in processes from scheduling to correlation has been a priority for the AuScope network since its inception and work in this area is also ongoing and significant (Lovell et al., 2017).

In its own right, as an individual network and as a significant part of the AUSTRAL sessions discussed in Section 2.4.3, there is also a focus on improving the usefulness of EOPs producible by the southern network sessions. This may be through the newly developed dynamic scheduling mode which will allow for flexible contributions from other global stations, as outlined in Chapter 5. Alternatively, it has been postulated that the uniquely high cadence of the AUSTRAL experiments combined with standard IVS observations in a VLBI time series, may provide new opportunities for the determination of sub-daily EOPs with VLBI (Plank et al., 2017).

In whichever capacity, the development and contribution of the AuScope network will be important for the future of geodetic VLBI operations and

results. It provides a significant capability for monitoring Southern Hemisphere sources and its development goals are diverse. In this work, however, we focus specifically on scheduling with AuScope and the ways in which this process can be used to more effectively run geodetic experiments. Utilizing the unique quality of the AuScope 12m array as a self-consistent array with near VGOS technical specifications, we test the resilience of traditional scheduling practice, as well as the new dynamic observing mode, to the implementation of an increased operational load. This is in line with both the goals of the institution, through pushing the limits of development, precision and innovation, as well as the geodetic community on the whole, by way of VGOS applications.

Chapter 3

Traditional Scheduling Method

The traditional method of scheduling is widely used and well proven. As the precision of EOP results depends on diurnal effects and nutation, it is common practice to schedule for periods of 24 hours or longer for geodetic experiments. In this case, many of these sources of error tend to cancel out and precision can be increased. However, often it is not always possible for a station to free a full 24 hour period for operation but shorter periods of time may be available. The analysis in this section was undertaken to determine whether there might be a point, less than 24 hours, where these effects are still non-critical and would, therefore, allow a network to contribute worthwhile results in a shorter observation period. That is, the overall aim is to improve efficiency without losing precision in geodetic VLBI. Predominantly, this section is focused on the AuScope network, but the results of such a study will have implications for other small networks sitting idle more than they need to be and also to heavily committed stations with small breaks between commitments hoping to further increase operational efficiency.

Hence, the most obvious test of the traditional scheduling method was to simply reduce the duration of a set standard schedule from 24 hours in a number of steps. However, a second test was conducted in an attempt to preserve the beneficial effects of observing for 24 hours but reduce the required observing time. The results of both these simulations are presented in this

chapter.

3.1 Simulation Parameters

VieVS is a scheduling and analysis interface for geodetic VLBI and is used throughout the community (see Section 2.2.3). As such, the simulations performed in this study were of a standard form for VieVS-based simulations, described in detail by Pany et al. (2010). In general, these rely on a schedule file, loaded into VieVS and subjected to three inbuilt processes: `vie_int`, `vie_mod` and `vie_sim` to generate simulated results which are compiled considering a range of environmental and observational effects. These can be iterated and subjected to a least-squares adjustment through `vie_lsm`. The considered schedule file can be produced by any scheduler, but in this case, VieVS was also used to create these schedules with the `vie_sched` scheduling process.

Due to the focus on AuScope results, the stations were constrained to be Hobart 12m (Hb), Katherine 12m (Ke) and Yarragadee 12m (Yg) and the AUSTRAL observing mode of 1 Gbps sampling (Plank et al., 2017) was defined. An effort to reduce variation in systematic effects was made and, as such, great care was taken to keep each test consistent with the next.

All schedules were set to commence on the arbitrary date of 12 MAR 2016 at UT 00:00:00 and a minimum source strength set to 0.8 Jy. In the analysis, station coordinates and EOPs were estimated once per session, while the quasar positions were fixed to their a priori positions. Clock values were estimated every 60 minutes and a white noise of 30 ps per baseline was applied. The troposphere model was defined to be $C_n [1e-7 \text{ m}^{1/3}] = 2.5$, $H [\text{m}] = 2000$, $ve [\text{m/s}] = 8$, $dh = 200$, $wzd0 [\text{mm}] = 150$, $vn [\text{m/s}] = 0$, and $dhseg [\text{h}] = 2$ with tropospheric zenith wet delays determined every 60 minutes and gradients every 360 minutes (Iles et al., 2017).

The schedule, once generated, was then used to produce 50 simulations to reduce any arbitrary fluctuations from the simulation process. The least

squares method was then applied to generate a result for each of the 50 cases. Single EOP and station coordinate results over the 50 simulations were defined through a standard deviation process. Similarly, a measure of error for each result was defined by the mean of the formal error produced by the simulation process over each case (Iles et al., 2017).

It is important to note here, that this style of simulation, as well as the simulation and scheduling parameters were all defined to reflect the current operation of the AuScope network. The goal was simply to develop and improve this network’s operational capability through scheduling. Therefore, the results of the following sections reflect this focus. Only after the completion of the work, has it become clear that the results of these simulations have obvious implications for a range of processes and institutions within the global geodetic community. Hence, the outcomes may be considered equally important on both local and global scales despite the fact that the following examples remain predominantly local (i.e. AuScope simulations).

3.2 Decreasing Duration Simulations

In an attempt to identify whether there is a duration less than 24 hours at which precision is only minimally affected and thus, to allow for an increased number of observations, a standard 24 hour schedule was decreased in duration by steps of 3 hours. Consequently, 8 schedules with durations of [03, 06, 09, 12, 15, 18, 24] hours respectively, were generated and the results simulated in the manner described by Section 3.1. These were created by consecutively removing blocks of 3 hours from the simulated 24 hour schedule. This potentially has significant implications for source availability corresponding to the start time throughout the day, so for the purpose of this study all schedules were commenced at the same time and date, as specified in Section 3.1. However, alternative days across the year have been tested and similar results were achieved (Iles et al., 2017).

3.2.1 Earth Orientation Parameters (EOPs)

After each session was produced using the standard method and parameterisation in VieVS, the resultant EOPs (xpol, ypol, dut1, dX and dY) and their formal errors were simulated. These were then able to be examined and compared using the MATLAB computing environment, both self-consistently and with values obtained from the literature. However, in the following discussion we focus primarily on the 3 Earth Rotation Parameters (ERPs): xpol, ypol and dut1 as indicative results for EOP precision in each case. Figure 3.1 shows these in terms of the standard deviation of the result and the mean of the formal error over the 50 simulations (Iles et al., 2017).

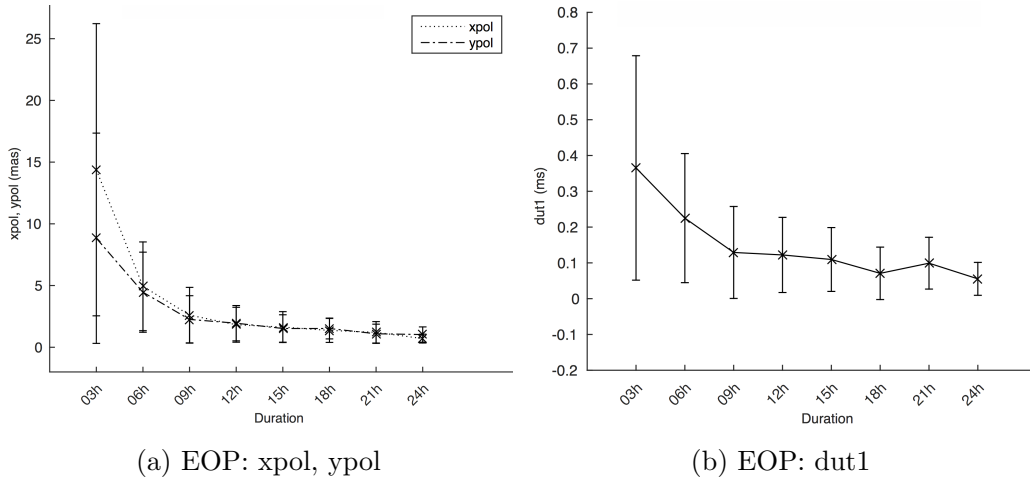


Figure 3.1: *ERP results in terms of the standard deviation of the result (delineated by \times) and the mean of the formal error (error bars) for each schedule duration (Iles et al., 2017).*

As mentioned previously, it is current standard practice in geodetic VLBI to schedule for 24 hour length sessions or longer. It is possible to see from Figure 3.1 that this is well warranted. The 24h result clearly produces the most precise results. Interestingly, it also seems apparent that there are a number of durations which produce results of a seemingly similar quality.

The shortest durations, 3h and 6h are immediately identifiable by eye as vastly different from even the standard of the other results. In fact, the 3h result is more than 20 times greater than the 24h result. However, for durations

longer than 9h the curve begins to level out. It is no longer immediately possible to determine what may be considered acceptable. If we once again consider the xpol result, the values for both 12h and 15h fall within 3 times the 24h result, defined here as a standard measure. The results for 18h and 21h, are similarly less than twice this 24h standard value. The other four EOP results also display such trends. From this, we could assume that 12 hours would be the minimum duration for worthwhile observations but 18 hours appears more desirable. However, these are only self consistent assessments.

To further justify this, we consider the IERS prediction capabilities for periods with no useable observational results. According to Bulletin A (IERS, 2017), the precision degrades as a function of time in days (D) since the last official IERS value. This is given by:

$$x, y = 0.68D^{0.80} \text{ [mas]} \quad \text{and,} \quad (3.1)$$

$$dut1 = 0.25D^{0.75} \text{ [ms]}. \quad (3.2)$$

Considering the polar coordinates (xpol and ypol), this corresponds to 0.39, 0.68, 1.18, 1.63 mas for 12 hours, 1, 2 and 3 days respectively. For the same parameters, our simulations produce differences ≤ 1.13 mas for observations 12 hours or longer and ≤ 0.67 mas for 18 hours. This indicates that it is possible to produce EOPs better than the IERS prediction capability after 2 missing days, observing with only the AuScope network for a period of 12 hours. With only 18 hours of AuScope observation, it is possible to produce better than the 1 day IERS prediction. Thus, it is reasonable to define a minimum of 12 hours or longer as sufficiently beneficial to make it worthwhile observing in what was originally idling time, although, 18 hours or longer would be more appropriate for better EOP precision.

It is important to note, however, that here we are comparing global EOP precision with simulated AuScope data. According to Plank et al. (2017), the AuScope network is not known for accurate EOPs due to its comparatively

short baselines. If we consider the current literature values for AuScope EOPs from the AUSTRAL experiments (Plank et al., 2017), the 24h simulation results are also seen to be consistent with these.

3.2.2 Station Coordinates

Station coordinates are produced in terms of x,y,z coordinates which, when added to a defined set of a priori coordinates, form the true station coordinates determined in the session. These were then converted to the more comparable root-mean-square (rms) station and baseline repeatabilities which are the primary measure for positional results. These results are particularly important for this study as there is a focus on improving the efficiency of geodetic operations with the AuScope network. Baseline repeatabilities are a main output of this network.

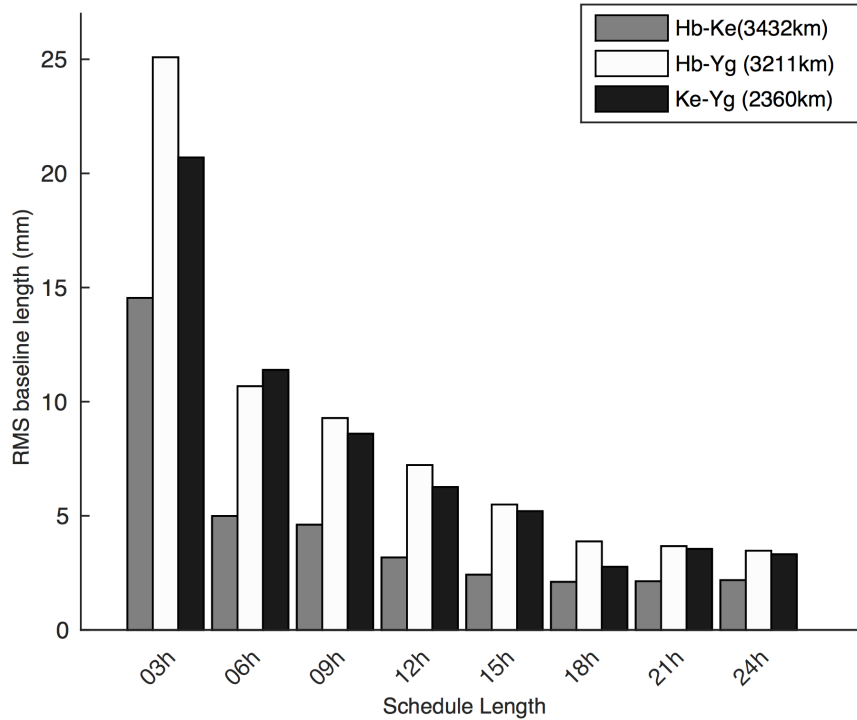


Figure 3.2: *Baseline repeatabilities rms (mm) for all baselines over decreasing time-steps, colour-coded to allow for identification of each of the 3 baselines.*

Figure 3.2 shows the rms baseline repeatabilities for each baseline in the network, simulated for the range of session durations. Here, it is possible to see a similar trend to Section 3.2.1. The best results are evidently produced for durations longer than 18 hours, although unlike with EOPs, it is not possible to conclusively state that the 24h result produces the best rms baseline length. Considering this figure closely it is also possible to identify periods where precision increases significantly between two durations. These are between the 03h/06h, 09h/12h, and 15h/18h schedules respectively.

All baseline repeatabilities with duration longer than 12 hours are well under 1cm, which was determined to be an approximately acceptable threshold, considering the previous performance of the network. However, those longer than 18 hours produce baseline repeatabilities between $\sim 2 - 5$ mm, a much more precise result (Iles et al., 2017). As in the previous section however, it is difficult to quantify this objectively. Hence, we consider the number of observations for each session on each baseline and compare it to what is known as the ‘Square-root of N Law’ as described by Equation 3.3 below.

$$\sigma = \frac{\sigma_i}{\sqrt{n}} \quad (3.3)$$

This relationship stems from the initial assumption that all observations are uncorrelated and affected by random Gaussian noise. If this is true, it would be possible to see an increasing precision in the derived result from many observations (σ), when compared to a single observation (σ_i) with an increasing number of observations (n). This has been proven to be of the form presented in Equation 3.3. When this is not observed, that is, when the number of observations does not correlate with the result in the form of $n^{-1/2}$, it is possible to assume there are other sources of error dominating the process.

Figure 3.3 shows this Square-root N Law compared to the baseline results of each duration simulation. Each baseline is separated and identifiable by a different line type. The simulation results are represented by \times . When the

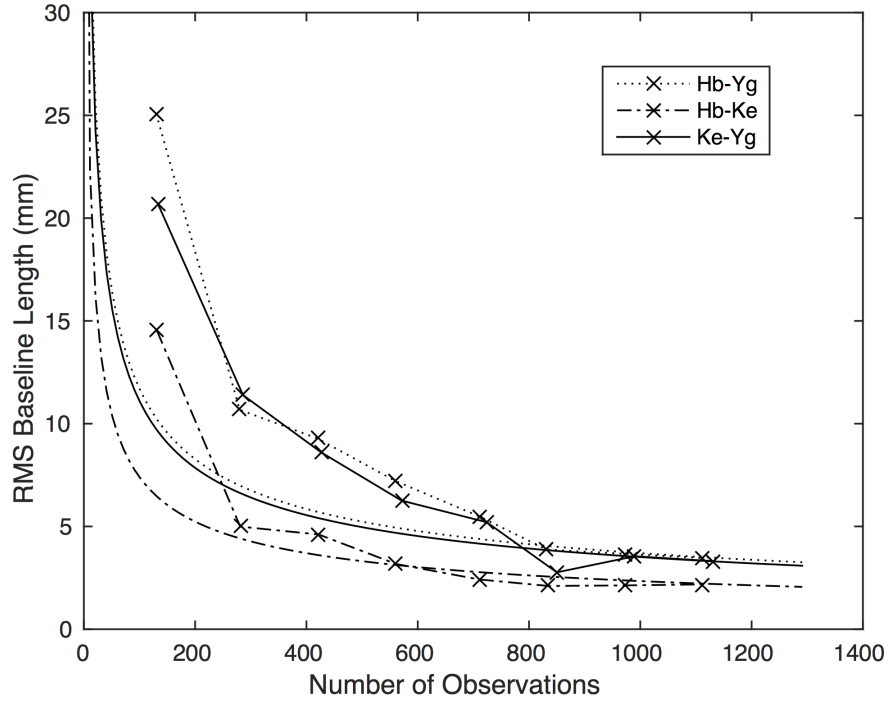


Figure 3.3: *The smooth curves represent the mathematical \sqrt{n} law for each baseline and its number of observations (n). The simulation results are indicated with a \times and joined to make a comparable line plot. The baselines are differentiable by individual dash patterns in both cases.*

experiment duration is longer, naturally the number of observations is higher. However, it is also possible to see that for durations of 18 hours or longer, there is good agreement between the results and the line of $n^{-1/2}$ on all baselines. The 12h and 15h results are beginning to diverge from the line of $n^{-1/2}$, but there is still some agreement, particularly for the Hb-Ke baseline. By the shortest duration (3h), the simulations clearly have other sources of error as there is little agreement with the Gaussian noise only case.

To apply this relationship between the number of observations and baseline results, consider Figure 3.4. This figure shows a combination of the results from Figure 3.2 and 3.3 with the $n^{-1/2}$ lines, overlaid on the original baseline results and the number of observations listed at the top of each bar. Figure 3.4 shows that the Hb-Ke baseline produces the best rms baseline repeatabilities. This baseline does not have the most number of observations in each session but

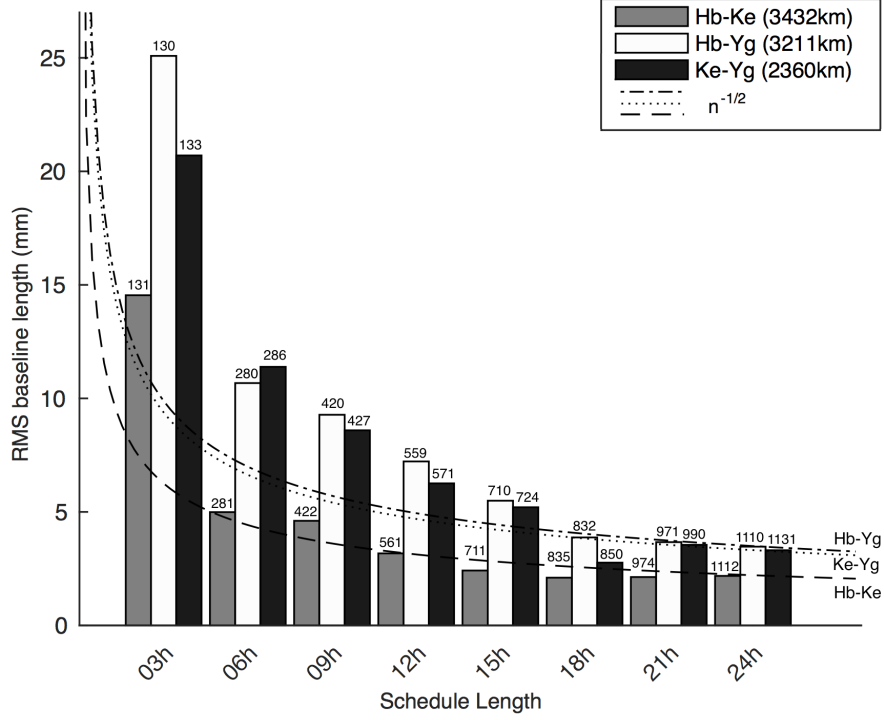


Figure 3.4: *Baseline repeatabilities rms (mm) for each of the 3 baselines from Figure 3.2. The lines represent the \sqrt{n} law for each baseline and its total number of observations (n) is stated above each bar (Iles et al., 2017).*

it does most closely follow the line of $n^{-1/2}$, indicating there are fewer other errors associated with the results even during shorter observing sessions.

Consequently, in considering this $n^{-1/2}$ relationship, it is possible to confirm the assessment that a minimum limit of 12 hours of observation might be acceptable if the aim is to make use of network idling time. However, 18 hours or longer will produce much more precise results for all baselines (Iles et al., 2017).

3.3 Interrupted Scheduling Simulations

The previous section’s simulation was focused on the viability of observing for shorter durations of geodetic VLBI sessions. It had implications for scheduling more experiments onto heavily committed and idle stations alike, with the end

goal to maximise the total number of global operations and help many stations transition to the continuous operation of VGOS. While this section shares the same implications, the application is very different.

While it is widely recognised that the precision of results from geodetic VLBI benefit from a full Earth rotation (observations of a full 24 hours), it is largely unspecified how significantly this relies on continuous observation throughout the session (Iles et al., 2017). In these simulations, we consider a variety of interrupted schedules over a 24 hour period. That is, a traditional schedule with blocks of missing observations. This could be an example of a network whose observations were interrupted to follow a ‘target of opportunity’, such as an astronomical event or spacecraft and satellite tracking, which is common for AuScope (e.g. Hellerschmied et al., 2017).

It could also be considered an example of some kind of practical fault. While it is highly unlikely that whole networks will drop out during a schedule due to unpredictable faults such as technical/operator errors or wind stows, it is still worth treating these simulations as an example of such. Although it becomes a rather pessimistic assessment, scheduling is a complex process of optimisation and, as such, losing even one station unexpectedly will negatively effect the precision of the entire experiment, especially in a small network such as AuScope, due to their relative geographical isolation.

Finally, intermittent observing is one of the proposed methods to reduce data overload during the transition to VGOS (Petrachenko et al., 2014). Hence, it is important to consider the relative implications that this type of observing will have on precision for the immediate future of geodetic operations (Iles et al., 2017).

In the previous section, it was shown that decreasing the total continuous observing time has an exponential-like degradation effect on the precision of EOP and baseline results. If this trend is consistent when the same time is lost sporadically during a 24 hour experiment, there exists a number of concerns for each of the 3 cases mentioned above. As such, a range of test schedules

were devised and results simulated in the manner described by Section 3.1.

3.3.1 Creating the ‘Cut’ Schedules

To create a range of schedules which would be both realistic and comparable to the analysis in Section 3.2, a variety of repeating and randomly generated patterns were devised based on a set number of missing hours. The original 24 hour schedule from Section 3.2 was used as the basis for these new, interrupted schedules. Parts of this schedule were removed in 1 hour increments until the total time removed added to 6, 9, 12 and 15 hours. These missing time brackets are directly comparable to the 18, 15, 12, and 9 hour schedule durations of Section 3.2 respectively. Figure 3.5 shows a graphical representation of these patterns.

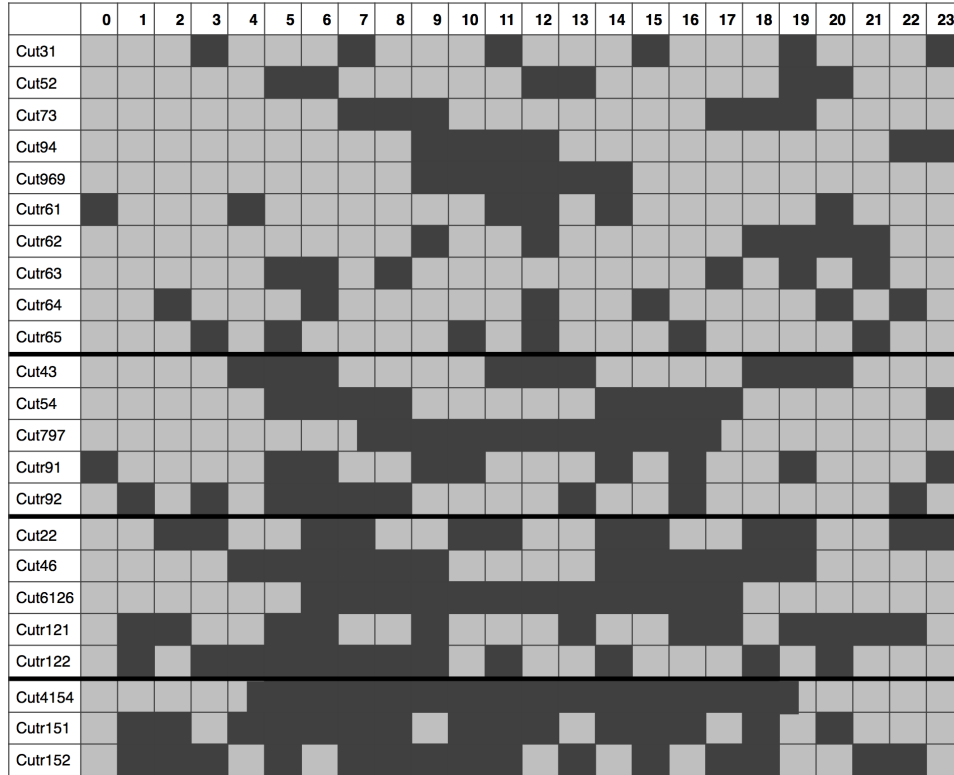


Figure 3.5: *Diagrammatic representation of missing hours (0-23) and the corresponding Cut ID designation. Black intervals correspond to time which is missing. A thick horizontal line denotes sections where total time removed changes: 6,9,12,15 hrs.*

From their method of creation, these new, interrupted schedules were identified by a CutID and became the ‘Cut’ Schedules. The numbers in the ID correspond to the pattern of operating hours. For example, ‘Cut31’ corresponds to 3 hours operating, 1 hour off. Random patterns are designated by the letter r, the number of hours removed and a sequential numeral for each test. See, for example, ‘Cutr61’ which corresponds to the first random test missing 6 hours (Iles et al., 2017). Dark squares in Figure 3.5 correspond to time when the network is not observing and thus, hours that were removed from the originally planned schedule.

3.3.2 EOP and Baseline Repeatability Results

The interrupted schedules were simulated and subjected to the same analysis as the schedules of reduced duration in Section 3.2. Interestingly, while they have a similarly decreasing total observation time, albeit over a smaller range, these simulations do not show a similar degradation in the precision of results. In Section 3.2, for both EOPs and baseline repeatability, precision appeared to decrease in an exponential-like manner. However, the interrupted schedules almost all produce results of a similar order to the original 24 hour schedule simulation. This is incredibly promising as it shows that geodetic experiments are very resilient to data loss over a 24 hour length experiment.

Figure 3.6 is of a similar form to Figure 3.1 from Section 3.2. Simply, from the y-axis limits on these plots, it is possible to see by eye the improved precision across each simulated scenario. However, as has been mentioned previously, these simulations are focused on the results of the AuScope network which does not geographically have the capability to produce particularly precise EOPs (Plank et al., 2017). We are primarily concerned with the precision of baseline repeatabilities, as this is a main product of AuScope experiments.

An example of the baseline results for the interrupted schedules is shown in Figure 3.7 for the Hb-Yg baseline. The line of constant rms baseline length shows the result from the original 24 hour schedule from Section 3.2. Despite

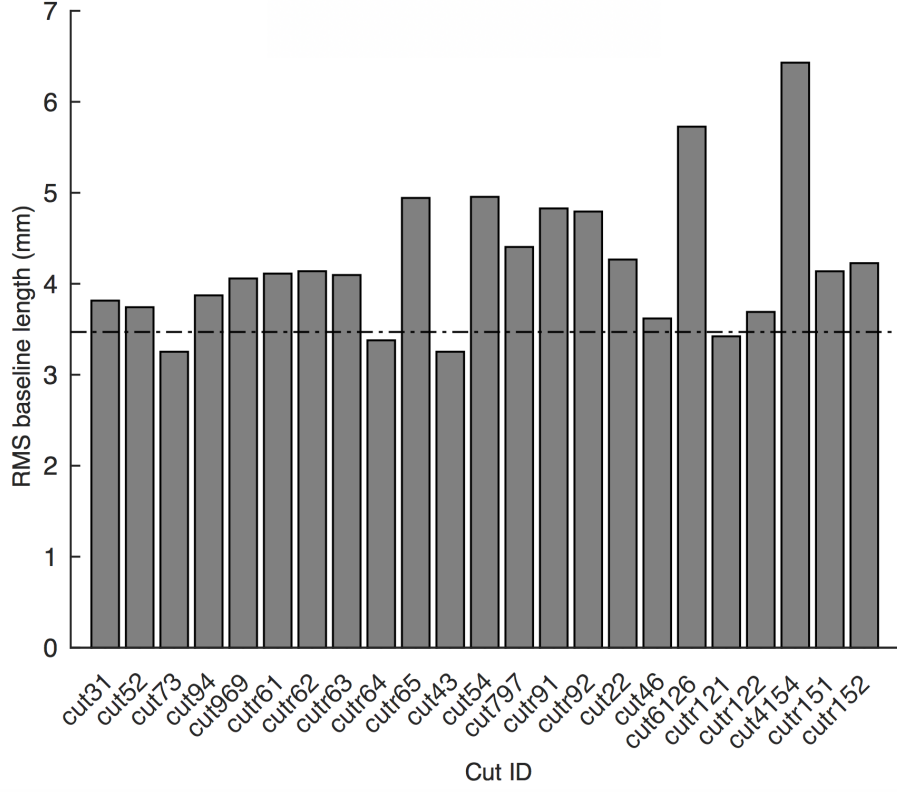


Figure 3.7: *Baseline repeatabilities for the Hb-Yg baseline over the variety of interrupted schedule test cases. Schedule names correspond to those in Figure 3.5. The dashed line represents the 24h result from the original schedules in Section 3.2*

over the 50 simulations. If the result coincides with the reference within its formal error, it is displayed as blue. Similarly, a yellow result is within twice the error and orange is a result within a factor of three. A red result corresponds to a value outside of three times the formal error, when compared to the reference schedule. Further, the EOP assessment is averaged across all 5 EOPs and it is important to note that the errors on these results are large (Iles et al., 2017).

The best results are not necessarily produced by the schedules with the most hours of operation, nor is there any clear distinction between whether the time is missing regularly or randomly. It is clear that long, central periods of inactivity do tend to produce worse results than their counterparts and

	0	1	2	3	4	5	6	7	8	9	10	11	12	13	14	15	16	17	18	19	20	21	22	23	Hb-Yg	Hb-Ke	Yg-Ke	EOPs
Cut31																									3.8	2.2	4.0	*
Cut52																									3.7	2.5	3.6	*
Cut73																									3.3	1.8	3.2	*
Cut94																									3.9	2.9	4.5	*
Cut969																									4.1	2.8	4.2	*
Cutr61																									4.1	3.7	1.9	*
Cutr62																									4.1	3.0	3.4	*
Cutr63																									4.1	1.8	3.2	*
Cutr64																									3.4	2.0	2.9	*
Cutr65																									4.9	2.4	4.6	*
Cut43																									3.3	3.3	3.8	*
Cut54																									5.0	2.8	5.0	*
Cut797																									4.4	2.5	5.3	*
Cutr91																									4.8	4.7	2.0	*
Cutr92																									4.8	3.0	4.9	*
Cut22																									4.3	2.1	3.5	*
Cut46																									3.6	2.1	3.6	*
Cut6126																									5.7	3.6	5.7	*
Cutr121																									3.4	1.8	3.4	*
Cutr122																									3.7	2.1	4.3	*
Cut4154																									6.4	4.6	7.8	*
Cutr151																									4.1	2.8	4.8	*
Cutr152																									4.2	2.8	4.4	*

Figure 3.8: Diagrammatic representation of interruption patterns from Figure 3.5. Baseline lengths rms (mm) are included and colour coded to identify consistency with Section 3.2’s original 24h result. Blue indicates good agreement, yellow and orange some agreement and red, no clear agreement. EOPs are coloured similarly based on the average over all 5 results.(Iles et al., 2017)

that schedules missing 15 hours are not as precise. An effort to identify the cause of these fluctuations is included in the following section, Section 3.3.3 but these results are sufficiently conclusive to state that, even when up to half the observing time is lost intermittently during a 24 hour experiment, it is still possible to achieve EOP and baseline results consistent with a full 24 hour experiment (Iles et al., 2017).

3.3.3 Is the Type of Interruption Related to a Greater Effect on Results?

This section briefly outlines an attempt to quantify whether there was some correlation between particular features of the interruption pattern and the quality of results produced. As mentioned previously, there seems to be some link between large continuous periods of non-operation in the middle of a

schedule and less precise results. For example, ‘cut4154’ and ‘cut6126’ which have 12 and 15 hours removed in one solid block produce the worst baseline results of all the schedules. This is also somewhat evident with the ‘cut969’ and ‘cut797’ results being some of the worst in their duration brackets. However, there are other similarly imprecise results which do not seem as easily correlated with any particular feature of the interruption pattern.

Hence, a range of possible contributing factors were considered alone and in combination to identify any situations to be avoided. These included the regularity or randomness of the missing intervals, the longest gap duration, number of gaps and whether time is missing at the beginning or end of the period. Figure 3.9 shows two examples of these.

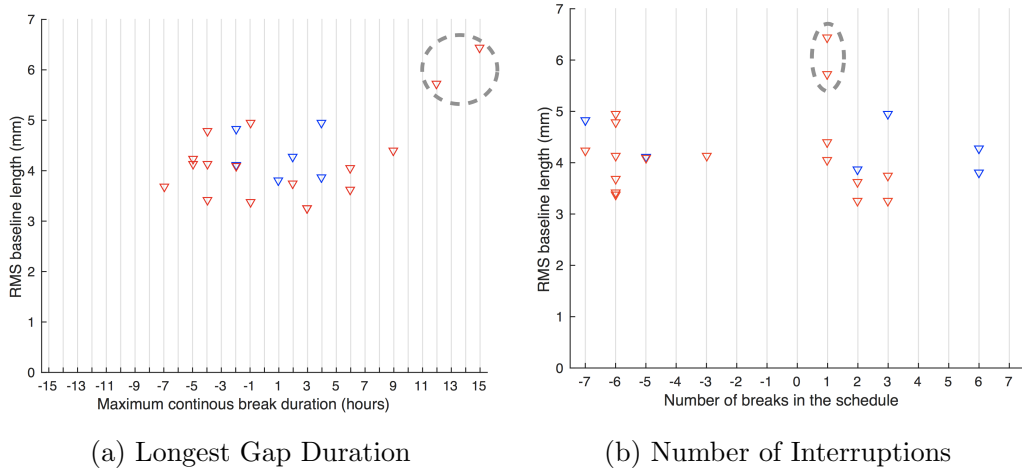


Figure 3.9: *Composite plots of schedule pattern attributes against the rms baseline length for the Hb-Yg baseline, as in Figure 3.7. Blue points are schedules which lose time at the start or end of the schedule, red are those that do not. Negative values indicate the interruption is random, while positive values are repeating patterns. The ‘cut4154’ and ‘cut6126’ schedules previously identified, are enclosed in the dashed region.*

These plots show a composition of a number of the possible contributing factors in order to most comprehensively identify any possible correlation. Figure 3.9a, predominantly considers the effect of break duration on the precision in rms baseline length. This is the maximum continuous time in the schedule that there was no observation. In a similar manner, Figure 3.9b considers the

total number of interruptions to the schedule. That is, the total number of times that the network stops observing. Other factors, such as the randomness of the interruption pattern and whether time is missing at the start or end of the schedule (therefore, it does not truly complete a full Earth rotation), are indicated in a true-or-false capacity. The randomness is indicated by multiplying the considered attribute value by -1 if the schedule is interrupted in a random pattern. Hence, negative values correspond to random patterns and positive values correspond to regular repeating patterns. The colour of each point indicates whether there is time missing from the start or end of the experiment: a blue colour indicates time missing; a red colour, no time missing.

From this figure, it is possible to see that no clear distinction could be made, aside from the already identifiable one. The ‘cut4154’ and ‘cut6126’ are the only points which seem to lie outside the cluster of results, particularly on the longest gap duration in Figure 3.9a. These are identified by a dashed region on each plot. The other attribute values are clustered with a mostly even spread of precision for each parameter. Hence, it is possible to state that as long as continuous periods of 12 hours or longer are avoided, there will be no correlation between the nature of the interruptions to a 24 hour schedule and the precision of its results. On the other hand, it is entirely possible that there is a more complex relation between any number of the factors considered here that was not identifiable with the set of patterns considered.

As a result, it is not possible to state with absolute certainty that there are no attributes of the interruption pattern which will effect the precision of baseline results. However, the analysis presented here does align with our statement in the previous section (Section 3.3.2). That is, that the precision of geodetic results is not heavily depended on the total observing time but rather the duration of the experiment session. Therefore, precision consistent with operating for a full 24 hour period of observation can still be achieved from a minimum of 12 hours of observation spread over a 24 hour period (Iles

et al., 2017). It is advisable, however, to limit long periods of inactivity for more precise results (Iles et al., 2017).

Chapter 4

The Dynamic Scheduler

The dynamic scheduler is an automated scheduling tool devised at the University of Tasmania to support the next generation of geodetic VLBI observations through the modification of the standard VieVS scheduler (Lovell et al., 2016). It has been developed primarily to enable greater flexibility and automation in scheduling VLBI observing sessions and forms the first stage of the overall ‘dynamic observing’ concept, which will eventually achieve the same goals over the entire geodetic observing process (Lovell et al., 2016).

The adjective ‘dynamic’ is used to indicate the constant change or activity in the process. That is to say, the dynamic observing concept and thus, the dynamic scheduler, has been designed to be constantly checking on the status of an operating network and to be able to adapt accordingly, in real-time, to any change in conditions. Naturally, if we consider the current standard of technological capabilities, true real-time adaptability is probably an idealistic situation. However, if we are able to check and adapt to changes even once during an observing session, we are already more flexible than the current practice where a schedule is usually produced days to weeks in advance and last-minute change notifications are usually sent by email and can be missed before the session starts. In fact, last minute changes are often avoided, even if it may mean poorer results, simply to avoid the risk of a missed email scenario.

In the following chapter, we focus on the practical aspects of using such an

automated scheduling mode. We also determine the most appropriate approximation for real-time updates and test the quality of its performance compared to the results of the standard scheduling method (e.g. Chapter 3). These are with the intent to show that the recently developed dynamic scheduler is capable of being used today to schedule observations immediately with no loss of precision, while significantly improving automation and flexibility in the network.

4.1 How Dynamic Scheduling Works

While the dynamic scheduling mode is notable because of its automation, it does also achieve the other main goals for dynamic observing: the ability to coordinate simultaneous observing programs; improve feedback throughout the system; be completely adaptable to last-minute changes and allow each site to have full local control by running operations on location (Lovell et al., 2016). Noting this, however, makes the process sound deceptively complex. In fact, the difference between the current standard practice and dynamic scheduling for individual participating stations, is small (see Figure 4.1).

Figure 4.1 shows a flow chart of the usual steps involved in scheduling for both standard and dynamic observing, as well as the approximate time line for each process. Whether a step is automated or requires the time and effort of trained personnel is indicated by a colour code: blue for manual, green for automation. As can be seen from this figure, the scheduling process itself remains the same but, between the two observing modes, many more steps are automated in dynamic observing.

This automation is what allows the dynamic capability for the schedule to be revised, adapted and reapplied throughout the experiment. The effects of this can also be seen in Figure 4.1 through the red time line. For any given standard experiment, the scheduling process can span many months, whereas, dynamic scheduling is completed in almost real-time. This increases both the

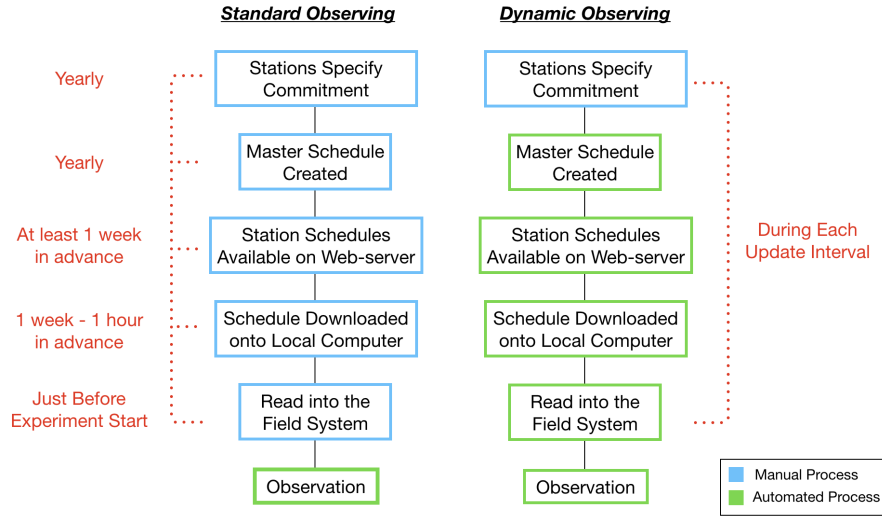


Figure 4.1: A flow chart of the scheduling process where standard observing is compared with dynamic observing. Automated processes are highlighted in green, while processes requiring an operator are in blue. A time-line is also included.

flexibility and resilience of the schedule to a number of last minute changes. Through automation, the dynamic observing mode is made more efficient in terms of time and human resources but fundamentally, the scheduling process itself is unchanged.

This automation is supported through two additional Perl programs running simultaneously alongside the PC Field System software at each station. These programs are small scripts which enable the dynamic nature of the process. One makes it possible for the field system to communicate with the dynamic scheduler and the other produces the interface from which an onsite operator can allow the station to join or leave the dynamic session.

As shown in Figure 4.2 (Lovell et al., 2017), this ‘red button’ script is the only manual step identified in the dynamic side of Figure 4.1. With this script, an operator at the participating station can specify commitment at any time before or during the experiment by simply pressing the ‘big red button’.

Dynamic scheduling relies on live information from participating stations to update the schedule file at specified intervals throughout the experiment. An

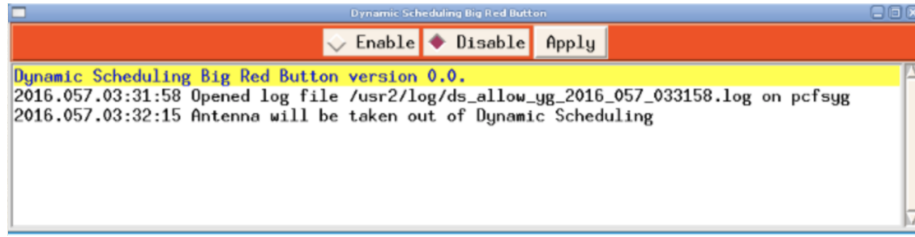


Figure 4.2: An example of the ‘red button’ program which will allow an operator to specify when a participating station will join or leave a dynamically scheduled session (Lovell et al., 2017).

operator at each individual station must specify when their station is capable of observing during the session. If the station is able to contribute for the entire duration, this step must only be performed once to enter the session. However, it is also possible to join and leave the session a number of times during the experiment.

	HOBART12	KATH12M	YARRA12M	HARTRAO	HART15M
Availability	Available	Available	Available	Unavailable	Available
Timestamp	2017-05-27 02:41:48	2017-05-27 02:41:57	2017-03-20 03:34:05	2016-08-17 05:42:26	2017-05-28 03:18:57
Status	slewing	tracking	tracking		
Schedule	r4795hb	r4795ke	r4795yg	none	none
Log	r4795hb	r4795ke	r4795yg	station	station
Halted?	no	no	no	yes	no
Scan name	160-0537	160-0538a	160-0538a	100-1431	339-1444
Next command	05:36:57	05:38:11	05:38:11	16:14:48	04:22:11
Source	0434-188	cta26	cta26		
Az	275.9946	276.4477	296.0773		
El	34.4179	30.0320	41.1463		

Figure 4.3: An example of the live page for dynamic observing. The details of the experiment and all participating stations can be quickly identified from this web-based summary page.

The station availability information from each station in the network is then coordinated by a computer in the operations centre. The VieVS-based dynamic scheduler subsequently produces an appropriate schedule file for the available stations and this is piped back to the respective field systems. A web server is used as an interface between the scheduling computer and participating

stations. In such a way, it is also possible to access a complete summary of the session from a web-based live page for monitoring purposes (Lovell et al., 2017), see Figure 4.3 for example. In this figure, a section of the live page is presented from during the IVS experiment R4795. Note that dynamic observing was not being undertaken at the time but the page still shows the relevant information.

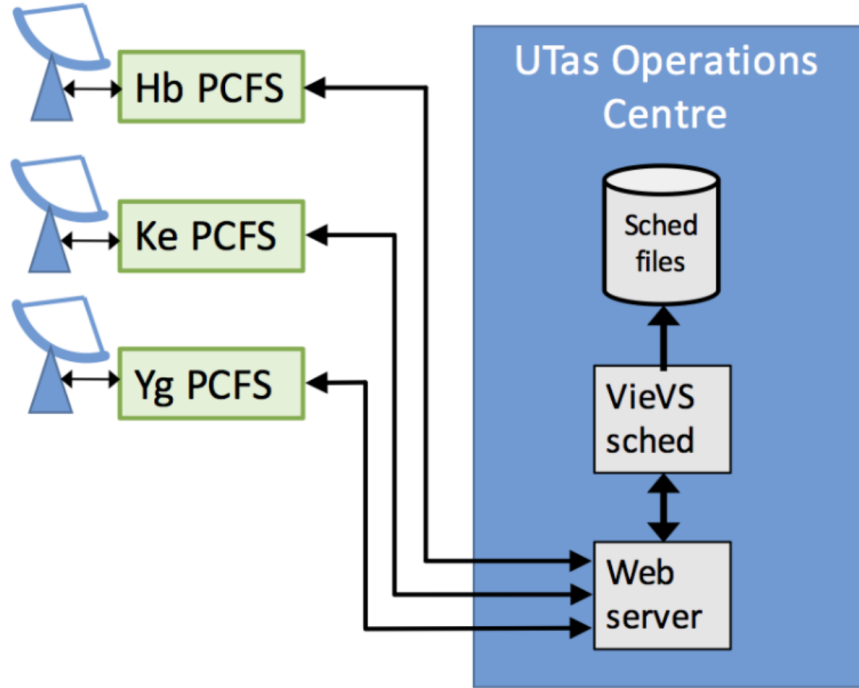


Figure 4.4: *A simple schematic of the information flow for dynamic scheduling in an AuScope experiment (Lovell et al., 2017).*

A simple schematic of the dynamic observing process is shown in Figure 4.4 for the case of an AuScope session. Here, operations are run from the UTAS control room. The participating telescopes send information about their operations to the field system software on the PCFS computers and are, in turn, controlled by the field systems. These are connected to the web server by the two Perl programs. An operator will send the instruction to enable or disable dynamic observing capability from the red button program on each PCFS computer to the web server. This will pass the station availability information to the VieVS dynamic scheduler. After a user specified interval,

the dynamic scheduler will then produce an updated schedule. This will be passed back to the web server and on to the telescopes via the field system (Lovell et al., 2017).

The session will run and repeat these steps until the total time has been observed and the process halted. As such, a station may drop in or out of a session at any time using the red button program. This will be accommodated for in the next schedule update and thus, the observations for all participating stations remain optimised. It is, therefore, also possible to make the decision to operate an entire network at very short notice, without requiring the time or presence of an operator trained in scheduling. Thereby, the dynamic scheduling mode should be entirely capable of significantly improving both flexibility and efficiency in VLBI experiments.

4.2 Considering the ‘Update Interval’

Dynamic scheduling depends on a piecewise method of compiling the schedule file as station availability is confirmed throughout the observing session. For each block, a new schedule is created with the current antenna slewing information carried over from the previous schedule.

The ideal situation would be to be able to produce automated, instantaneous, real-time scheduling. For the present, however, we must consider some practical limitations. For example, we must consider that scheduling is a complex process of optimisation in itself which takes both time and computing power to complete. As well as this, even with the most modern technology, data transfer rates are far from instantaneous to all station locations. As such, for current uses of the dynamic scheduling technique, there should exist an optimum period of time which is as close to real-time as possible without an unnecessary drain on resources.

This is a user specified ‘update interval’, after which the dynamic scheduler will check station availability and generate a new section of the schedule file

to pass to the participating stations. If the update interval is chosen correctly, it will maximise operational efficiency in terms of both time and cost, as well as the flexibility and adaptability for experimentation in terms of target and station selection. Thus, dynamic scheduling will be able to make the best use of all available resources in the community. However, as this is a completely new scheduling mode for geodetic VLBI, appropriately choosing this update interval has no precedent.

In this section, we compare EOP and baseline results produced by simulations with the dynamic scheduler to the simulations from Chapter 3 which are indicative of the standard scheduling mode. The primary area of concern is whether the same level of precision can be achieved with a dynamically updating schedule as with the standard schedule and to what extent we may reduce the update interval to bring the process as close to real-time scheduling capability as possible.

4.2.1 Simulation Results - EOPs and Baseline Repeatabilities

The simulation results considered in this section are all based on schedules created by the newly developed, modified VieVS dynamic scheduler but were produced using the same methods outlined in Section 3.1. For a similar 24 hour experiment, twelve different options for the dynamic update interval were considered. As the total observing time must currently be some multiple of the update length, these were defined as: [24h, 12h, 6h, 3h, 2h, 1h, 30m, 15m, 10m, 5m, 2m, 1m] (Iles et al., 2017).

The 24h update interval is not truly dynamic as the entire schedule falls within one dynamic interval. However, it was included to provide a direct comparison with the results of the 24 hour schedule used as a standard for the traditional scheduling process from Chapter 3 (Iles et al., 2017).

The 24h results were used to confirm that dynamic scheduling is theoretic-

cally capable of producing results consistent with the standard precision of the current process. This is important as the dynamic scheduler runs on a modified version of the VieVS software to provide for the increased automation. The subsequent update intervals of decreasing length were then designed to challenge the smallest possible limit of update interval, in line with the aim of real-time scheduling capability (Iles et al., 2017).

As in the previous chapter (see Section 3.3), baseline lengths were considered as the primary area of comparison since we are concerned with results of the AuScope network. Figure 4.5 shows the baseline results produced for the dynamic scheduling simulations with varying update interval.

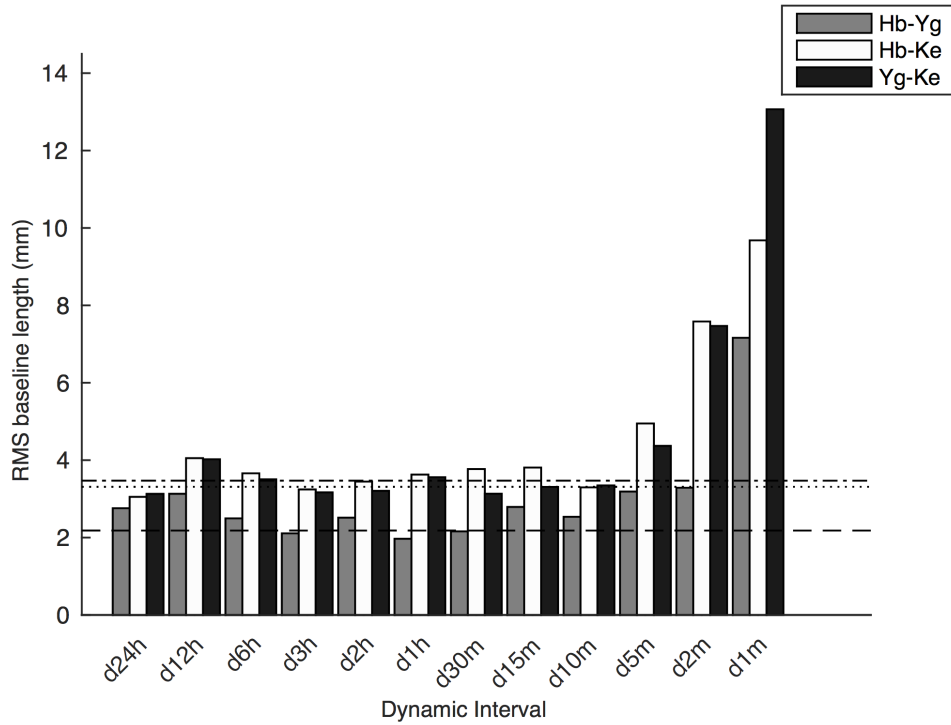


Figure 4.5: *Repeatabilities for all baselines over decreasing dynamic interval. For each baseline, dashed horizontal lines denote the 24h result from the original simulations in Section 3.2.*

By comparing the dynamically produced 24h result to the dashed lines, which show the baseline results from Section 3.2, and remembering that, for these simulations, baseline results are considered consistent within ± 1 mm

it is possible to evaluate the dynamic scheduler against the standard mode of scheduling. The dynamically produced 24h result is clearly consistent for all baselines. Hence, it is possible to assume that dynamic scheduling should indeed produce results comparable with the standard method of scheduling (Iles et al., 2017).

Reassuringly, the baseline results for update intervals significantly less than 24 hours also appear to deliver consistent results. It is only for update intervals of approximately 5 minutes or less, that these results start to display a degradation of precision which increases sharply as the update interval decreases (Iles et al., 2017). For consistency, we also consider the EOP results. Although, it is once again important to note that these are simulated for the AuScope network which does not produce the best quality EOPs (Plank et al., 2017). These can be seen in Figure 4.6.

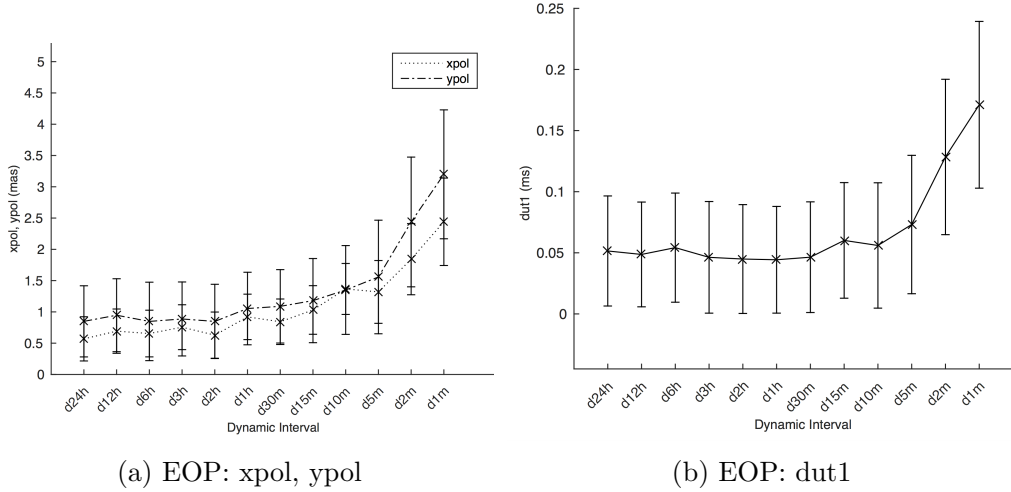


Figure 4.6: *ERP results in terms of the standard deviation of the result (delineated by \times) and the mean of the formal error (error bars) for each schedule duration. This time produced by the dynamic scheduler and with a number of varying update intervals.*

The EOP results produced are also in agreement with the results from Section 3.2 for most update intervals. They also begin to degrade significantly at an update interval of 5 minutes. From this, we can feel confident in asserting that there is some process which is ‘breaking’ the dynamic scheduler’s capa-

bility for these smaller update intervals. This is subjected to further analysis in the next section. However, it is possible to conclude, at this point, that the dynamic scheduler seems to give good results down to an update interval of approximately 10 minutes. As such, it is significantly more flexible than the current scheduling mode and is able to produce similar results with an increased level of automation.

4.2.2 Variation of Precision with Dynamic Scheduling

It is possible to see from the results in Section 4.2.1 that the most significant variation in precision occurs as the update interval decreases. From both EOP and baseline results (see Figures 4.5 and 4.6), this appears to become significant at approximated 5 minute update intervals. Once again though, the precise moment of change is difficult to identify from just these plots.

Theoretically, we may expect a degradation in precision as source repetition errors should become increasingly dominant with increasingly rapid schedule updates. As discussed in Section 2.2.2, this is because the scheduling process has a range of built in priorities for identifying sources to target, such as required slewing time, source strength and the area of sky.

These are particularly important because, for small update intervals, the number of different sources in the optimal area of sky is also small. This is due to the fact that the telescope does not have time for many sources to transition from visible to not observable, or for long periods of slewing. As the dynamic scheduler simulated here does not take into account the sources observed in the previous scheduling block, the probability of the same sources being observed in a subsequent schedule block increases for small update intervals. Thus, source repetition is increased without limit.

A short update interval also leads to the prioritisation of higher strength targets, due to these sources requiring less time on source per observation. This significantly constrains the number of available sources. Hence, scan numbers increase and the number of different sources observed decreases. These

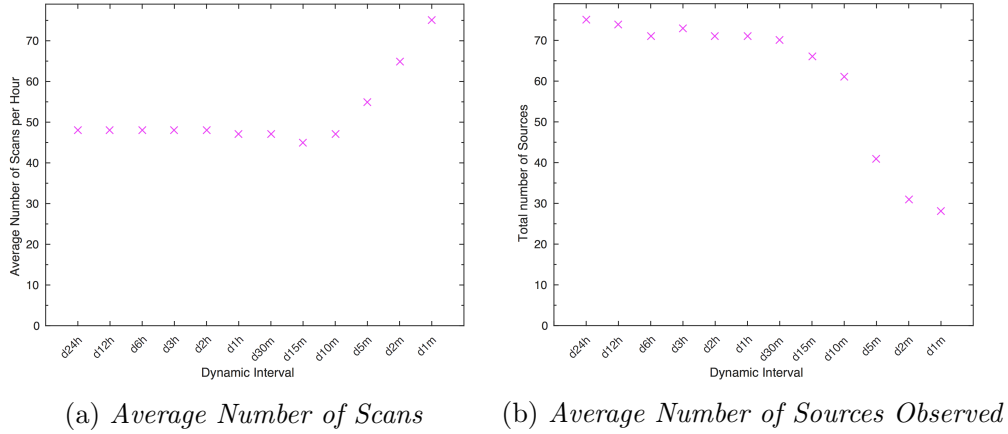


Figure 4.7: *The average number of scans and the average number of different sources observed over 24 hours at different dynamic update intervals.*

are both factors which could become critically detrimental to the precision of geodetic results and are plotted for the update interval simulations in Figure 4.7.

Figure 4.7a represents the behaviour of scan frequency as the dynamic interval decreases and, correspondingly, Figure 4.7b shows the average number of different sources observed for each simulation. These two plots clearly demonstrate the expected behaviour and further provide an explanation for the significant degradation in precision observed in Section 4.2.1 for shorter update intervals. It can be seen in Figure 4.7 that the major change occurs at approximately the 10 minute interval rather than at 5 minutes which was determined by eye from the results of Figure 4.5 and Figure 4.6. This is most evident from Figure 4.7a where scan numbers per hour take a sharp increase after the 10min point. The total number of observations on each baseline is also relatively constant at approximately 1100/24h until it increases significantly for intervals less than 10 minutes (Iles et al., 2017).

The detrimental effects of both these factors can be simply decreased with more rigorous conditions imposed on the scheduling process. The first operational version of the dynamic scheduler used for these simulations, does not correct for sources observed in the previous schedule block. Subsequently, a

revised version of the scheduler has been developed with this capability added. As such, with the latest version of the dynamic scheduler, it should theoretically be possible to achieve flexibility on the order of 5 minutes or less. This is yet to be tested.

How the dynamic scheduler copes with the retrospective addition of scans into the idle time of the fastest stations in the network, or ‘fill-in scans’ (as discussed in more detail by Sun et al. (2014)), also poses an interesting question for further investigation as we continue to push the limits of dynamic scheduling.

The main problem associated with these very short update intervals, however, is not due to some nuance in the scheduling process itself but with our current technology. As discussed in Chapter 2, geodetic VLBI is currently struggling with increasing data rates. While it is conceivably possible to improve the dynamic scheduler itself to be able to schedule in intervals ≤ 1 min, this does not assist with passing that information quickly and seamlessly to the participating stations and the associated equipment. So, in practice, the goal of real-time scheduling still seems excessive for the moment.

From these simulated results it is evident that the dynamic scheduler, even the current version that does not correct for sources observed in a previous block, is capable of achieving results consistent with the current method of scheduling. These results, as well as the scan and source number analysis, appear to correspond with update intervals of approximately 10 minutes or longer. Hence, it was possible to determine that an update interval of 15 minutes would be sufficient flexibility to account for changes in station priorities or availabilities mid-experiment (Iles et al., 2017).

This suitably accounts for the major variation of precision observed in Section 4.2.1 where there is a clear trend for precision degradation toward shorter update intervals. However, if we remove the smallest intervals and focus primarily on the baseline results which are more consistent with the standard mode of scheduling (as in Figure 4.8), it is possible to observe a less significant

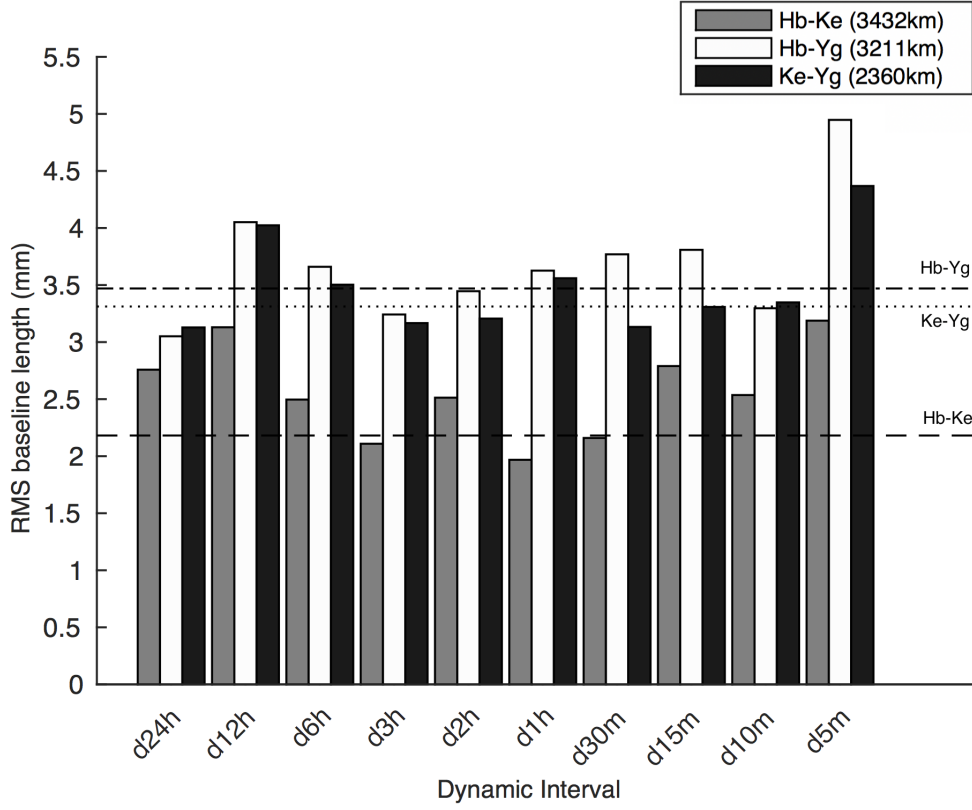


Figure 4.8: A version of Figure 4.5 to exclude the shortest update intervals. Repeatabilities for all baselines over decreasing dynamic interval. For each baseline, dashed horizontal lines denote the 24h result from the original simulations in Section 3.2 (Iles et al., 2017)

variation in precision between the update intervals tested. This variation does not seem predicated on update interval length, baseline or baseline length, nor does it seem apparent in the scan number or number of sources plotted in Figure 4.7.

This was potentially attributed to an effect from the total number of observations and a variation from the Square-root N Law, in a similar way to the manner by which precision could be seen to decrease in the simulations of Section 3.2. However, this was not proven to be the case, as any variation in the total number of observations was not closely correlated to a variation in baseline repeatability or divergence from the line of $n^{-1/2}$. The only significant divergence from this line occurred at approximately 5 minutes, supporting the

previous assertions regarding a minimum appropriate update interval.

Instead this variation is attributed therefore, to inbuilt schedule or simulation parameters. The VieVS scheduling process itself works with one set of predefined global parameters, such as source list, minimal source strength, minimal and maximal scan length and weighting options. Any of these could be influencing some small precision fluctuation. In addition, despite the results having been derived statistically over 50 simulations to reduce random error, there is still some simulation related variation in the results. Thus, it was determined to be a non-critical artefact with no immediate bearing on the successful use of this and subsequent versions of the dynamic scheduler (Iles et al., 2017).

4.3 Quality Check

In the previous section, it was made clear that dynamic scheduling is capable of producing a precise standard of results for any update interval longer than 10 minutes and an interval of 15 minutes was suggested as a good balance of flexibility with practicality. In the following section, and subsequent chapters 15 minutes is the update interval set for all dynamic scheduling.

With no loss in precision observed when dynamically scheduled results are compared to the standard mode of scheduling, it seems possible to assert that the dynamic scheduler could be used immediately to provide automation and a significant improvement in experiment flexibility. In this section, we present further tests to confirm that this is indeed the case for experimental applications at the specified update interval of 15 minutes.

4.3.1 Simulation

One of the main benefits to dynamic scheduling is the ability to schedule and commence observing sessions at short notice, without requiring the presence of a skilled operator to sufficiently schedule the session. This is a large part of the

motivation for AuScope as it will definitely impact the ability of the network to make more efficient use of idling time between experiments. The ability to dynamically schedule experiments using the AuScope network is also a simple transition, since the array is already centrally operated from one command center (Iles et al., 2017).

In Chapter 3 the analysis was predominantly concerned with assessing whether it is possible to reduce observation time for standard geodetic experiments. This also has implications regarding the different scheduling decisions have the capability to reduce antenna idling time in a productive manner. Here, we return to the considerations of Section 3.2 where a standard 24 hour schedule was reduced by a time-step of 3 hours at a time to determine a minimum worthwhile operation window. It was found that observations of 12 hours or longer would be a better use of time than simply letting the network sit idle. However, the practicalities of the standard scheduling method mean that 12 free hours would, in fact, not be a sufficient window if the time were to become available at the very last-minute. Additional time would be required for a skilled operator to produce a schedule and pass it on to the field systems, as well as to prepare the equipment for operation. With dynamic scheduling, only the normal setup procedures would need to be accomplished while the schedule produced itself. This could therefore be done by any operator, not necessarily skilled in the area of scheduling, and in a shorter period of time.

Therefore, as a first level quality check, the simulations from Section 3.2 were repeated using the dynamic scheduler. Instead of creating a full 24 hour schedule and removing hours, the dynamic scheduler was run and the network made available or unavailable accordingly to produce the set of [03, 06, 09, 12, 15, 18, 21, 24] hour schedules. These were then simulated in the method of Section 3.1 to produce both EOP and baseline repeatability results. Although, once again we are primarily interested in the baseline results for AuScope.

As can be seen from Figure 4.9, the same trends for baseline repeatabilities are produced. The results are also consistent with those found in Section

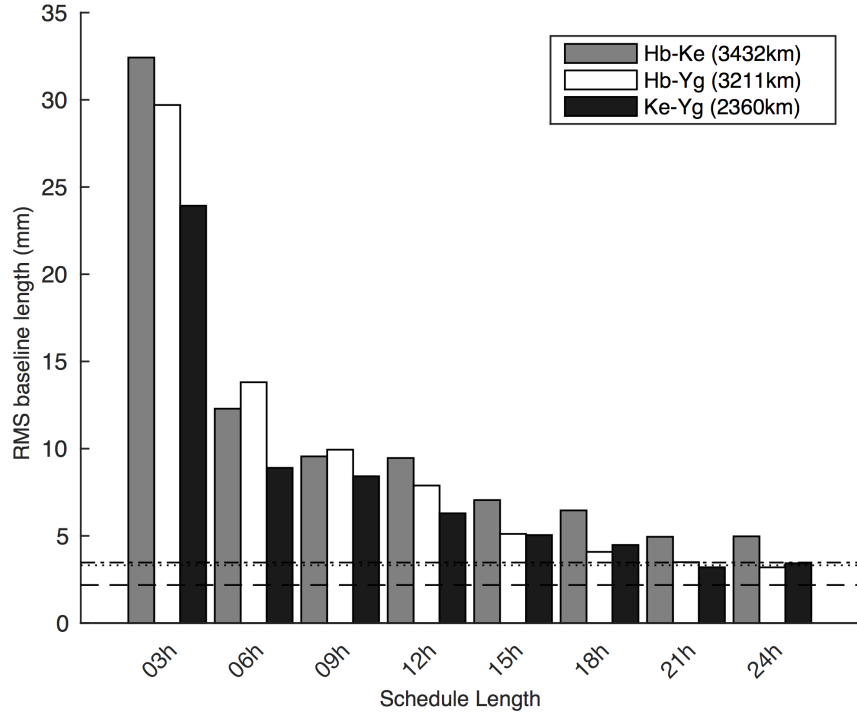


Figure 4.9: *Baseline repeatabilities for all baselines over decreasing time-steps, as in Section 3.2.2. This time produced with the dynamic scheduler. For each baseline, dashed horizontal lines denote the 24h result from the original simulations in Section 3.2.*

3.2. This confirms our earlier assertions about the benefit of dynamic scheduling, particularly for AuScope but also for other stations looking to increase their operational commitments towards continuous observing. For example, if scheduled maintenance is completed ahead of time, an operator can simply make the call to begin observing. For a single telescope, this would require joining an existing experiment but for small, easily coordinated networks, the operator must simply be sure that the time available is more than 12 hours. With dynamic scheduling, there is no need to predict when this time will become available (Iles et al., 2017).

4.3.2 Observation

Consistent with the update interval analysis in Section 4.2.1, a 15 minute update interval was also used for the experimental proof-of-concept tests for

dynamic scheduling outlined in table 4.1 (Lovell et al., 2017).

Session Name	Antennas	Observation Range in 2016 (day/UT)	Extracted Session Time Ranges
ds239	Hb Ke Yg	240/0126 - 242/0250	240/0126 - 240/2359 241/0000 - 241/2359
ds258	Hb Ke Yg	257/2312 - 258/2237	257/2312 - 258/2232
ds275	Hb Ke Yg	275/0027 - 276/2300	275/0027 - 275/2359 276/0000 - 276/2300
ds288	Hb Ke Yg	288/2346 - 291/0354	289/0300 - 290/0259 290/0300 - 291/0354
ds317	Hb Ht Ke Yg	317/0100 - 319/0201	Awaiting correlation
ds337	Hb Ht Ke Yg	337/1942 - 339/2147	337/2322 - 338/2247 338/2248 - 339/1846
ds351	Hb Ke Yg	350/2349 - 354/0003	351/0001 - 351/2359 352/0000 - 352/2359

Table 4.1: *Dynamic scheduling proof-of-concept observation sessions in 2016 (Lovell et al., 2017).*

These tests were undertaken mostly with the AuScope network with assistance from the Hartebeesthoek Observatory [Ht] in South Africa for a number of sessions. The baseline results produced were also found to be consistent with results of the standard AUSTRAL experiments (Lovell et al., 2017). This is a significant validation of dynamic scheduling as a legitimate mode for geodetic VLBI scheduling. It also proves our simulation results experimentally.

As a further quality check for the simulation method, a number of the observed schedule files from these sessions were simulated in the method described by Section 3.1. This also produced results consistent with the dynamic observations, in the same way that the simulations of Section 3.2 were found to be consistent with the standard of AUSTRAL results. Hence, it is possible to have confidence in the assertions outlined by this chapter and the next, regarding the capabilities of dynamic scheduling as an automated scheduling mode.

The dynamic scheduler is able to produce results consistent with the precision of the current standard scheduling mode, but with increased automation

and adaptability. It is able to be used to commence an experiment at the last-minute without devoting additional time and resources in the form of a skilled scheduling operator and can currently adapt to a change in conditions within the participating network at a flexibility of 15 minute update intervals. However, this is not the limit to its capability to improve operations and precision in geodetic VLBI.

Chapter 5

Simulating a Global Network

In the previous chapter, we were mostly concerned with the dynamic scheduler as a newly developed scheduling mode and in assessing whether it would be capable of rivalling the current scheduling mode for precision while increasing automation and flexibility within current experimental parameters, particularly for the AuScope network. This chapter builds on that research and, instead, focuses on how the dynamic scheduler may present new capabilities for global geodetic experiments.

One of the main benefits of the dynamic scheduling mode is that it allows individual stations the flexibility to control when they join or leave an experiment in almost real-time. In this chapter, we define an arbitrary global test network to consider the implications of augmenting the AuScope network with additional global stations. This would validate using the dynamic scheduling mode as a means to provide last-minute support to an already scheduled session from a wider network and thus, increase the total number of geodetic observations worldwide. Such a capability would also be significant to the operations of the AuScope VLBI array, since it offers the chance to increase baseline lengths, an important consideration for precise EOP results.

In the following discussion, we show that the current version of the dynamic scheduler is already capable of successfully managing such a global network and attempt to ascertain the extent to which it may be used to improve AuScope

EOP results with minimum interruption to the operational commitments of other stations.

5.1 Creating a Global Network

In order to test the capability of the dynamic scheduling mode for dealing with a global network in a flexible and automated manner, one must first define such a global network. In this section, the aim is to define a network which is sufficiently spanned on the globe to provide a significant increase in baseline length in comparison to the relatively small Australian network. However, this network needs to do more than span the greatest global volume as indicated by Malkin (2008). For our interest, it must also provide some diversity in global position. That is, there must be some stations which provide significant increases in N-S and E-W baselines, as well as some stations which are close enough to Australia to consider the extent to which baseline length must be increased for a noticeable change in precision.

As such, a variety of IVS stations were considered to form the test global network and be assessed in the following simulations. The final network was determined to be comprised of the three AuScope Australian 12m telescopes, considered in the previous chapters, as well as stations at Hartebeesthoek, Ishioka, Fortleza, Onsala, Warkworth and Wettzell. The details of these stations and their location can be found in Table 5.1 below. They are also displayed geographically with some examples of baselines identified in Figure 5.1.

This selection can be considered completely arbitrary, in terms of the actual process of dynamic scheduling. Any number or variation of IVS stations could have been selected, however, the selection of these particular stations is based, in part, on a variety of contributing factors, such as a diverse continental contribution (see region column of Table 5.1), baseline length and direction (see example baselines in Figure 5.1), as well as stations who often offer to collaborate with the AuScope network at short notice for target of opportunity

Antenna	Abbreviation	Location	Region
Hobart 12m	Hb	Tasmania, Australia	AuScope (Asia-Pacific)
Katherine 12m	Ke	Northern Territory, Australia	
Yarragadee 12m	Yg	Western Australia, Australia	
Warkworth 12m	Ww	Warkworth, New Zealand	Asia-Pacific
Ishioka	Is	Ishioka, Japan	
Onsala 60ft	On	Onsala, Sweden	Europe
Wettzell	Wz	Wettzell, Germany	
Fortleza	Ft	Fortaleza, Brazil	The Americas
Hart 15m	Ht	Hartebeesthoek, South Africa	Africa

Table 5.1: *The test network of global stations used for dynamic scheduling simulations and their locations. The AuScope stations are shaded in grey to more clearly identify the additional IVS stations.*

or technological development sessions. The main priority, however, was to have as complete a global coverage as possible, with a relatively small number of stations for efficiency in developing test simulations.

In the two subsequent sections, all and part of this network is used to challenge the automation and adaptability of the dynamic scheduling mode in a more global context. This is particularly important as expanding the network has a number of complex scheduling implications. For example, in the global context, the likelihood of ‘subnetting’ in the schedule is increased. This is an automated decision in the scheduling process whereby the full network is divided into smaller sub-networks to better achieve the scheduling priorities discussed in Section 2.2.2, primarily due to joint visibility. Subnetting, and correspondingly effective subnetting, is a complicated but important part of current scheduling procedures. As the dynamic simulations have been completed without manually changing any scheduling priorities or parameters, it is important to confirm that the dynamic scheduler is capable of managing these larger networks with the same level of competency as it manages the 3 or 4 station networks that were previously tested.

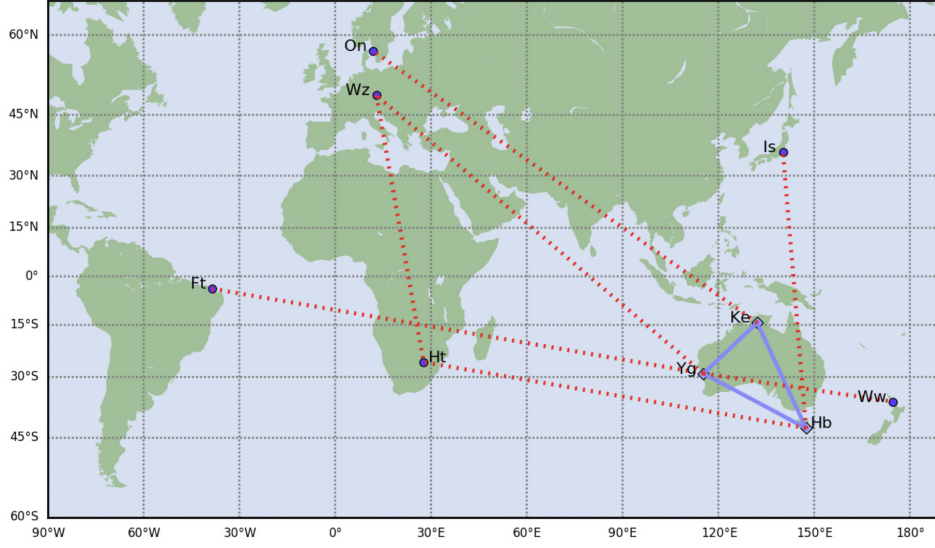


Figure 5.1: *Geographical locations for test stations in the defined global network. Some baselines are illustrated by a dashed line to highlight improvements to baseline length and thus, global volume.*(Iles et al., 2017)

The results of these global simulations will also allow us to determine whether the dynamic mode of scheduling can be used to provide more effective collaboration between global geodetic partners. Seamless, short notice collaboration is a factor which we believe will become increasingly important during the transition to full VGOS operation in the near future. This is particularly with respect to the need to increase total observing time at all stations (e.g. Altamimi et al., 2016). For example, dynamic scheduling makes it possible for a station to contribute to an existing network’s experiment when a local operator finds it is free and able to operate. Whether this may have a benefit to the quality of results produced from the assisted session, is one of the major ideas considered in this chapter.

5.2 Augmenting the AuScope Network with Global Stations

As has been mentioned previously, the AuScope network does not produce particularly precise EOP results due, predominantly, to its relatively short baselines (Plank et al., 2017). It has been postulated that one of the main benefits of dynamic scheduling, for AuScope in particular, would be the capability for other global stations to assist at short notice and for unspecified durations during a predominantly AuScope coordinated experiment. Consequently, there would be an increase in baseline length which would ideally lead to more precise geodetic results to contribute to the global reference frames.

In this section, we consider a number of network simulations with the stations specified in the test global network (see Section 5.1) to determine first, whether this is indeed the case and consequently, to what extent a contribution is required in order to significantly improve results. At this point, it is important to note that the dynamic scheduling process was not changed from the work of the previous chapter. There were no manual corrections to preset scheduling priorities in order to account for a mutual visibility requirement when selecting sources for stations separated by long baselines. The current version of the scheduler also does not do this automatically. In the future, it is hoped that this will be one of the major improvements to the intelligence of the automation in the dynamic scheduling process. The same simulation analysis method from Section 3.1 was also used in order to produce comparable results.

The networks scheduled and simulated in this section are documented in Table 5.2. These are simple combinations of the stations selected in Section 5.1 added to the 3 AuScope antennas, ranging from one additional station to all additional global stations. Sample standard R1 (R1779) and R4 (R4777) experiment schedules were simulated to provide a measure of the ideal precision in EOP results. The station combinations were also not selected randomly. There were a variety of selection factors. The primary consideration was max-

Network (Including Hb+Ke+Yg)	Volume (Mm ³)
+Is	4.396
+On +Wz	17.74
+Ht +Wz	44.28
+Is +On +Wz	40.78
+Ft +Wz	47.08
+Is +On +Ww	62.09
+Ht +On +Ww	84.21
+Ft +Ht +On	124.11
+Is/Ht +On +Ww	120.02*
+All (8h each)	228.81*
+All	228.81
R1	351.61
R4	376.55

Table 5.2: *Volume of the global network test cases spanned onto the surface of the globe.*

*- *This is the volume of the total network, however, not all stations observed for the entire duration. (Iles et al., 2017)*

imum global volume and minimum additional stations. This is due to the work of Malkin (2008), who has shown that it is not simply baseline length which is important for precise EOPs. Instead, EOP results are strongly related to the volume on the surface of the globe which is spanned by the network (Malkin, 2008). Hence, the global volume is also displayed in Table 5.2.

Most of these networks are not truly making use of the dynamic capability of the dynamic scheduler. They are simply scheduled for the full 24 hours of the session to determine the extent to which AuScope would require assistance to improve EOPs. However, this tests how detrimentally the results may be affected by the fact that the scheduler does not prioritise mutual visibility for participating stations. There are only two schedules in this section which make a change of stations and, thereby, make use of the dynamic capability. These are listed in Table 5.2 as +Is/Ht+On+Ww and +All (8h each). In the first case, Ishioka was switched with Hart 15m halfway through the experiment, giving a 12 hour contribution from each. In the case of +All (8h each), the stations were randomly assigned a pair and these pairs contributed for 8 hours of the experiment before switching to the next pair. The station pairs were as

follows: +Ft+Is, +Ht+Wz, +On+Ww.

Figure 5.2 shows the results of these tests in terms of ERP results in a similar manner to all EOP analysis in previous sections. From this figure, it can be seen that the R1/R4 experiments with the largest network and global volume do indeed produce the best EOP results. However, it is important to note that the R1/R4 use a different (smaller) sampling rate (256 Mbps) and consequently, are not directly comparable. This is why they are identified by a different symbol in Figure 5.2. It is also evident that the full global network defined in Section 5.1 can be used to produce similar results to the R1/R4 experiments. It would be ideal, however, to use dynamic scheduling in this situation to achieve the most precise results with the least possible disruption to any assisting stations. Hence, asking for 24 hours of assistance from 6 other stations is not exactly practical and the commitment becomes similar to existing R1/R4 experiments (Iles et al., 2017).

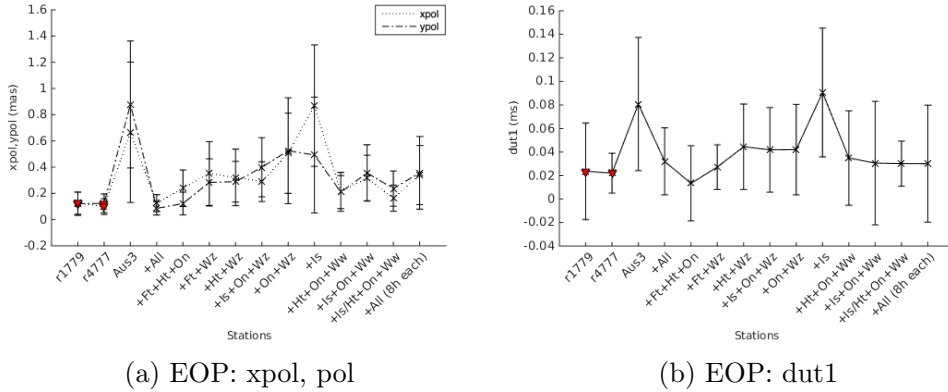


Figure 5.2: *Indicative ERP results for the range of global networks tested with the dynamic scheduler, presented in terms of the standard deviation of the result and the mean of the formal error as in Section 3.2. R1 and R4 results are also simulated for comparison but are not directly comparable due to the sampling rate (Iles et al., 2017).*

This is not a concern however, as all the test networks appear to produce results significantly more precise than the Aus3 result which represents the EOPs of the AuScope network from Section 4.3. As such, it is possible to support the claim that the AuScope network's EOP results are poorer due

to its relatively small global volume. The conclusions of Malkin (2008) are also supported as, following the full network, the next best EOP results are produced by the largest network in which all stations observe for the longest duration. It can be seen from Figure 5.2 that contributions from only two additional stations can make a difference of almost 50% to EOP results. With the addition of 3 assisting stations, specifically chosen to maximise the global volume of the network, it is almost possible reproduce the standard of the global R1/R4 experiments (Iles et al., 2017).

Subsequently, we are justified in applying the more dynamic qualities of the dynamic scheduler to networks with only 2 or 3 additional stations, as seen through the two examples here. These are also individually indicative of the two methods to augment the global volume of small networks.

Consider the +All (8h each) case. This only requires each additional station to contribute 8 hours of operation but, over the session duration, it will cover the full volume of the test global network. Such a contribution could be served by stations only observing during the day while staff were already on site. From Figure 5.2, it is possible to see that the +All (8h each) results produce a significant improvement to the Aus3 standard but do not achieve the same level of precision as the fully observed global sessions (+All, R1, R4). It did, however, produce a result of the same order as the 24 hour contributions from 2 stations with large global volume and this, in turn, could potentially be improved by a more intelligent selection of observing pairs (Iles et al., 2017).

The second case +Is/Ht+On+Ww is an example of using dynamic scheduling to switch between two stations mid-session. This requires a longer operational commitment from all participating stations but less stations are required to devote time. In this situation, it would allow two stations to share commitment to the experiment, regardless of whether this is to maximise global volume or due to time constraints at one or both of the switching stations. For example, switching between the two European stations (On/Wz) could maintain a European contribution for the duration of the session, if either station

was unavailable for a full 24 hour experiment (Iles et al., 2017).

On the other hand, switching between stations such as Ishioka and Hart 15m in the manner presented here, could serve to maximise the global volume. Ishioka has a significant improvement in the N-S baseline length, whereas Hart 15m is primarily an improvement in the E-W direction. Considering Figure 5.2, the results for both xpol and dut1 from the switched simulation is better than both cases where Ishioka or Hart 15m contribute for the entire 24 hours (+Is+On+Ww and +Ht+On+Ww). The ypol result is consistent with the larger volume of individual addition (+Ht+On+Ww). Thus, it is possible to assert that global precision of EOP results can be significantly improved with the capability of dynamic scheduling to change stations mid-session without needing a full 24 hour contributions from many stations (Iles et al., 2017).

The only simulation which produces a similar result to the Aus3 value is that which comes from the addition of only 1 station from the global network. This confirms the concerns mentioned earlier regarding the dynamic scheduler’s inability to consider joint visibility. The addition or removal of stations in the schedule is fully automated based on the station availability, as described by Section 4.1. A human scheduler would naturally give consideration to joint visibility when adding a more distant station to the network and may change scheduling parameters accordingly. Since the current dynamic scheduler does not do this, the assisting station will not contribute significantly to the observations if joint visibility is low. Hence, we see a similar result to the case where only the original network is observing (Iles et al., 2017).

It is theoretically possible to correct for this by improving the automation processes of the dynamic scheduler. However, the current scheduler already shows a significant capability for improving AuScope EOP results with the addition of global stations, even without a consideration for joint visibility. From the results presented in this section, the dynamic scheduling mode can be seen to successfully coordinate the resources of a global network. It is capable of automatically and dynamically managing on-the-spot changes in station

availability and therefore, the size and potential of the network. Utilising both of these properties, the dynamic scheduler can become a tool to significantly improve the precision of results produced by the AuScope VLBI array, through the flexible addition of 2 or more assisting global stations. While some care must be taken to consider global volume, it is possible to switch between stations mid-session and produce similar or better quality EOP results (Iles et al., 2017).

5.3 Intermittent Contribution of Support

The previous section demonstrated it should be possible to significantly improve the precision of EOP results produced, by augmenting the AuScope network with only 2 additional global stations. However, many of the simulated networks from Section 5.2 did not fully consider the improved flexibility introduced by the dynamic scheduling mode to session planning. For example, it would still be relatively simple to schedule the previous section’s test cases with the standard method of scheduling. In this section, we endeavour to further explore the dynamic capabilities of using this mode to observe with a global network in a manner which would be incredibly difficult to manage with preplanned scheduling.

The following simulated results were produced using only one subset of the global network, the AuScope array plus 2 assisting stations (+Ht+Wz). Here, we suppose that the 3 Australian antennas are observing with Hart 15m in a joint experiment, as is relatively common. Wettzell is assumed to have some other operational commitments but may be able to spare some observation time for a global collaboration. As such, it allows us to begin to consider the effects of intermittent contribution from an additional station to the existing sessions of a small network. Dynamic scheduling would make this a simple process for any station with the dynamic scheduler scripts installed on their field system computer (as described by Section 4.1). If the results are

promising, short notice and intermittent contributions to existing experiments would be an efficient and flexible manner to steadily increase operational times, as well as the precision of global geodetic results.

This particular network was selected due to its large global volume as well as the fact the Hart 15m has already contributed to the dynamic observing proof-of-concept experiments, mentioned in Section 4.3.2. Hart 15m is also an important choice geographically as it provides significant joint visibility with the European stations that is difficult for the AuScope network to achieve alone. The intermittent contribution patterns were also not randomly selected. Instead, the analysis of Section 3.3 was used to develop a number of test cases which should balance precision of results (as produced in Section 3.3) with the perceived disruption to operations at the assisting station.

A selection of 8 interruption patterns from Figure 3.5 were determined to represent the contribution of Wettzell to the session. These were managed using the dynamic scheduler to switch availability on and off in the specified pattern. For reference, these can be seen in Figure 5.3. A dark segment means Wettzell does not observe, whereas a light segment indicates Wettzell's participation in the session.

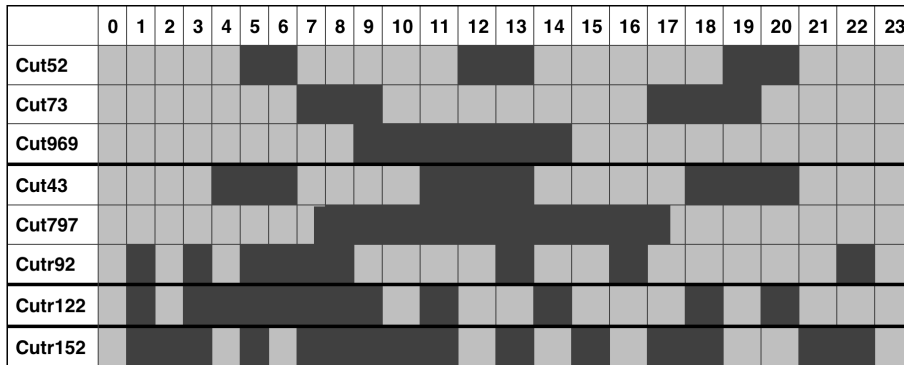


Figure 5.3: *Diagrammatic representation of Wz observing hours (0-23) created from Figure 3.5 for dynamic observing. The corresponding CutID designation is used to link patterns with Section 3.3. Black intervals correspond to time which is not observed. A thick horizontal line denotes sections where total operational time changes: 18,15,12,9 hrs.*

The EOP results are presented in the same manner as the previous sections, in terms of the ERP results plotted in Figure 5.4. The R1/R4 experiments are once again simulated and their results included for comparison, despite the difference in sampling rate. The Aus3 result from Section 5.2 is also included, as is the case where both stations contribute for the entire duration of the experiment.

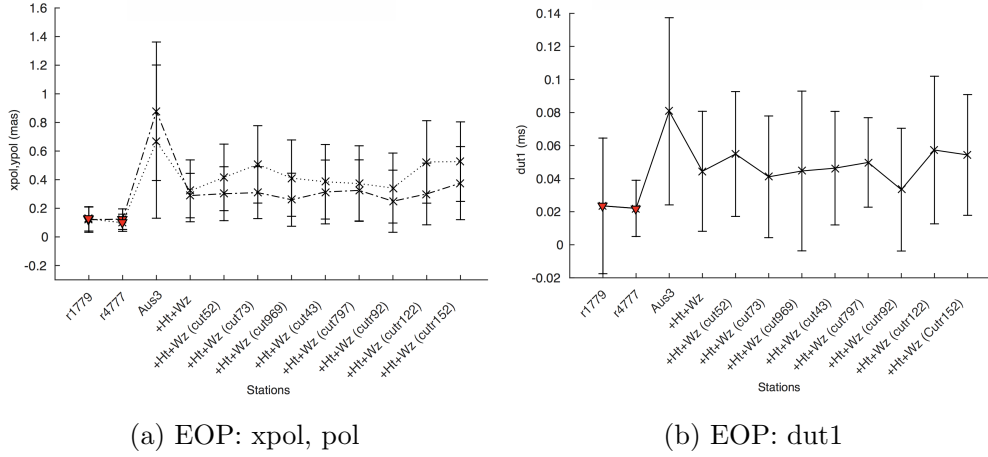


Figure 5.4: *Indicative ERP results for the range of dynamic interruptions to Wettzell's contribution, as tested in terms of the standard deviation of the result and the mean of the formal error in line with Section 3.2. R1 and R4 results are also simulated for comparison but are not directly comparable due to sampling rate. CutID numbers correspond to Figure 3.8 and Figure 5.3 (Iles et al., 2017).*

It is possible to see from this figure that each of the dynamically augmented sessions produce results which significantly improve on the precision of AuS-cope only EOPs. In fact, as we would expect from the analysis of Section 3.3, it seems that each case is able to produce a result which could be considered consistent with Wz observing for the full 24 hour duration of the session. Also unsurprising, based on that section's analysis, is that precision is worse for the simulations where both global stations participate for the least time.

This is significant because it once again demonstrates that precision in the dynamically scheduled experiments follows similar trends to the current standard method of scheduling. More importantly however, it shows that through

dynamic scheduling, it is possible to coordinate interruptions throughout a session, either planned or otherwise, and to use them in such a way as to efficiently optimise station commitments for the worthwhile use of global geodetic resources.

The assertions of Section 5.2 are proven to hold true, even when introducing an intermittent contribution from one of the assisting stations. That is, these results demonstrate that with the assistance of only 2 additional stations, even with diverse commitments, it is still possible to significantly improve the precision of AuScope EOP results. For example, a similar improvement to precision can be achieved through a station contributing for a total of 18 hours with 3 short breaks as if the same station contributed two periods of 9 hours with one long break in between. If we were to take this a step further and combine these results with the results of switching stations in Section 5.2, where a change mid-session between Ishioka and Hart 15m produced better results than either session in which they each contributed for 24 hours individually, it is reasonable to assume that intermittent contributions could also be shared between a range of stations and thus, lessen the burden on each assisting station while still further improving global EOP precision.

In this way, it is possible to see that we are only just beginning to consider the potential dynamic scheduling might provide to our capability for coordinating global geodetic experiments. The test cases simulated in this study are only the first ideas for how we may wish to use this increased automation and flexibility in the scheduling process and have yet to be attempted observationally. However, each clearly shows that the dynamic scheduling mode is more than capable of improving efficiency, flexibility and resilience to last-minute changes for the existing types of global and small network geodetic experiments, as well as future collaborations. For the AuScope network, at the very least it will provide a valuable tool to make more effective use of idling time at short notice, improve the precision of EOPs and enable more efficient target of opportunity sessions to be coordinated.

Chapter 6

Conclusion

A number of simulation studies have been presented here with the aim to consider the implications of changing the widely accepted, current practices for scheduling geodetic VLBI experiments. The capabilities and limitations of the standard scheduling mode were explored, as well as a newly developed automated scheduling mode in the form of dynamic scheduling, with a particular view to maximising efficiency, observation time and, consequently, the output of precise geodetic results. This was primarily focused on the results and operations of the AuScope VLBI array, however, these results will have significance for many parts of the global geodetic community as we begin the transition to VGOS operations. The potential of the dynamic scheduler is of particular importance.

In this, the final chapter, we revisit the project motivation to assess the completion of all research aims; summarise the most significant results; and present our conclusions with a view to the development of scheduling practice for geodetic VLBI in the near future.

6.1 Revisiting the Project Motivation

This project was predominately motivated by a desire to make better use of the AuScope network. As a small, independently coordinated, Southern VLBI

array, the potential of this network is large. Despite this, it often spends time idling between planned IVS contributions and general maintenance, for a range of reasons. It is, therefore, an institutional goal to increase the total number of observations completed by the network through improving the efficient use of all resources, but not at a loss of geodetic precision.

As such, automated and effective scheduling had been identified as an avenue to achieve these goals, since it has been proven to make a significant difference to the precision of results, the time and cost efficiency of an observing program and the flexibility of a station to adapt to changing conditions. These goals are also not limited to the AuScope network and hence, the outcomes of this project have implications for other stations with similar allocation problems, as well as for the wider geodetic community during the transition to continuous observation in the VGOS era of operation.

The VGOS goal of continuous 24/7 operation is posing many concerns for the geodetic community at present. How to manage the required large amount of human resources and data to be transferred globally is currently the topic of much discussion and research worldwide (e.g. Nothnagel et al., 2016b). As a precedent for this study, we proposed that to achieve such a goal would require all stations to push the limits of their current capabilities or even necessitate a new mode of observing entirely. Hence, we prioritised both these options as distinct avenues for research. It also appears that one may influence the other and both may be required to sufficiently improve efficiency and the management of resources in order to cope with truly continuous operation while continuing to produce high quality results throughout the intervening transition years.

A solution to the overwhelming data transport and resource management problem remains illusive, so we predict that the results presented here and the others which will inevitably follow it, are to become increasingly important. Thus, the motivation for this study is double-layered. On one level we are concerned with improving the output of the AuScope array both in volume

and in the quality of results, through more adaptable scheduling opportunities. However, on a broader level, these results should contribute to the wider changes in the application of geodetic VLBI which is ongoing globally.

6.2 Summary of Results

In this study, simulation results were considered in the form of the EOPs x_{pol} , y_{pol} , $dut1$, dX and dY ; as well as station coordinates presented in terms of the baseline repeatabilities. These were compared across a range of schedules for a clear determination of which scheduling situations could produce results with an acceptable level of precision. This was consistently compared with the values of current experimental results and the results produced by simulating a schedule for a standard 24 hour session. This section outlines the major findings for the current standard mode of scheduling, as well as for the automated mode introduced in the form of the dynamic scheduler which have been considered in the project.

6.2.1 Standard Scheduling Mode

For the schedules produced with the standard scheduling mode, two methods of reducing the time required for operation were considered. The first was to reduce the total observing time by iteratively removing blocks of 3 hours at a time from the end of an initial 24 hour schedule. This was in an effort to determine whether it would be worthwhile operating the AuScope network if a period of 24 hours was not available for a standard geodetic session. Secondly, a full 24 hour period was maintained to preserve a complete Earth rotation, which is important for precise results, but intermittent observations were made during this time. This would enable breaks for maintenance or other short observational commitments as well as simulating the effects of unexpected errors on a session, such as wind stows or equipment malfunction. It is also a representation of one of the proposed methods to reduce data overload as we

move towards continuous VGOS operation.

For the continuous, shortened observations, it was found that in the event that a full 24 hours is unavailable, an observation period of 12 hours or longer would produce usable EOP and baseline results to a standard better than the IERS prediction capability for 2 days of no observations. If a period of 18 hours or longer was available, this would be capable of producing EOP results better than the IERS prediction capability after only 1 day. As such, it would be more advisable to observe for 18 hours if possible, but a minimum of 12 available hours would make it worth observing with the AuScope network. Continuous sessions of less than 12 hours are not recommended, even if available, as the precision of geodetic results is determined to be critically affected, since degradation increases exponentially with reduced observation time.

This is not the case for an interrupted 24 hour session. Instead, this method of observing is noted to be particularly resilient to loss of observation time. Even after a variety of intermittent periods of no operation in the network for up to 12 hours, the precision of results can still be seen to be consistent with the quality of a standard 24 hour continuous period of observation. As would be expected, due to the relationship between covering a complete Earth rotation and precision, the worst results are produced when there is a long continuous period of inactivity in the schedule (such as 9 - 12 missing hours in a row). Hence, it is advised to limit long breaks if choosing to observe in this manner. There is also some fluctuation in the precision of results which is not explainable by a simple factor of reduced observation time. This is potentially attributed to some complex relationship between the attributes of the pattern for missing observations and the precision of results but the nature of such a relationship was not identifiable based on the simulations completed within this study.

Regardless, it has been shown to be entirely possible to achieve usable geodetic results when observing for less than the current standard of 24 continuous hours. This has current significance for fitting more sessions onto the

AuScope and other network’s operational calendars. If possible, it is better to aim for full 24 hour length sessions with intermittent observation for more precise results. This also supports the plans for transition to VGOS, as such sessions are still able to produce the current standard of results.

6.2.2 Dynamic Scheduling Mode

A new, automated dynamic scheduling mode was developed in line with the ideas of dynamic observing (Lovell et al., 2017). This mode was subjected to rigorous consideration in order to test the best method of its application in the form of scheduling current experiment types. A first look at the improved capabilities and limitations, in terms of the adaptability and automation of the dynamic scheduling mode was also completed. This was predominantly through an attempt to flexibly augment the AuScope network with a range of IVS global stations in order to improve the precision of EOP results for the traditionally baseline-limited array.

For the version of the dynamic scheduler tested in this study, it was found that an update interval of 15 minutes would be ideal for maximising both precision of results and practical constraints. This is because there appears to be a significant degradation of precision after an interval of approximately 10 minutes. Until that point, however, the dynamic schedules show no degradation in precision when compared to similar standard schedules. Hence, the dynamic scheduling mode can be used immediately and should be able to replicate the current standards.

As the dynamic scheduling mode does not require a schedule to be produced and distributed well in advance and is capable of checking the status of all stations in the network every 15 minutes and responding accordingly, it is capable of doing this with significantly increased adaptability to last-minute changes, even those which may occur mid-session. It also does not require an operator trained for scheduling to create the schedule before the session starts. In this way, the increased automation improves efficiency in the distribution of

time and human resources, as a dynamically scheduled experiment can begin as soon as the antenna is prepared by a standard operator. This is of particular interest to the AuScope network which is already coordinated from a central command centre and aims to efficiently increase its operational capability.

It was also shown that it is indeed possible to augment the AuScope network with additional global stations for improved EOP results. This is a process which is made particularly seamless through the use of dynamic scheduling to manage the participation of assisting stations. It seems that a significant improvement can be observed without a correspondingly significant contribution from a large number of stations, such as the common R1 and R4 experiments. An improvement of approximately 50% can be seen with the addition of only 2 assisting stations contributing to an AuScope experiment. With the full global network of 6 stations tested, the results produced rival those of an R1/R4 standard.

Making further use of the dynamic capabilities inherent in this mode of scheduling, it was possible to see that improvement is largely related to global volume, not necessarily to station position, so it is even possible to switch assisting stations throughout the session for similar or better results. An interrupted contribution from one of the 2 additional stations was also seen to deliver improved EOP precision. Thus, it is possible to suppose that only small contributions from a range of other global stations could be used on a regular basis to significantly boost the quality of EOPs generated by AuScope observations.

The results of this study clearly show that the dynamic scheduler forms a significant tool which can improve the geodetic operations of the AuScope and global networks. It is particularly capable of facilitating short notice experimentation or collaboration to improve global geodetic results.

6.3 Conclusion and Future Outlook

This project has been focused on revisiting the scheduling process, primarily to increase the total number of observations and quality of results from the AuScope network, moving into the next era of geodetic VLBI. The development of a new, automated mode of scheduling was also an important contributing factor. EOPs and baseline repeatability results were considered for a range of simulations and compared for an improved understanding of the capabilities and limitations of different scheduling methods.

The results presented here are significant for the continuing development of standard scheduling practice as well as for increasing automation throughout the entire observing process. The fact that VLBI faces enormous challenges with the implementation and transition to VGOS is no understatement. It will be absolutely necessary for the entire community to seek for a solution to the overwhelming amounts of data which will need to be shipped globally and the resources required at every station for continuous operation (Nothnagel et al., 2016b).

In this study, we have identified a number of ways that the current mode of scheduling can be pushed to achieve the goals of increased operation without a significant loss of precision. We have also considered the implications of using the automated, dynamic scheduling mode on standard experiments and started to consider new ways it can be useful for coordinating geodetic observing sessions to great success. The results show that the dynamic scheduler presented here, can have a positive impact on the adaptability and flexibility of VLBI experiments. It will allow participating stations to efficiently increase their observational commitments and can, in turn, trigger the development of greater automation in the next stages of observation such as data transport, correlation and analysis.

As far as AuScope is concerned, effective scheduling will be a significant part of coping with the challenges faced in the near future of geodetic opera-

tions. To achieve the ambitious goals of the institution itself and the IVS in the form of VGOS's 24/7 operational capability, a comprehensive understanding of the limits and capabilities of both the standard and dynamic modes of scheduling will be essential. The results contained in this study provide only one step on the path towards achieving these goals.

References

- Altamimi Z, Rebischung P, Métivier L, Collilieux X (2016) ITRF2014: A new release of the International Terrestrial Reference Frame modeling non-linear station motions. *J Geophys Res* 121: 6109-6131.
- AuScope (2012) AuScope: An organisation for a national earth science infrastructure program. <http://www.auscope.org.au>
- Böhm J, Schuh H, Tesmer V, Schmitz-Huebsch H (2003) Determination of Tropospheric Parameters by VLBI as a Contribution to Climatological Studies. *VGI – Österreichische Zeitschrift für Vermessung und Geoinformation* 91: 21-28
- Böhm J, Böhm S, Nilsson T, Pany A, Plank L, Spicakova H, Teke K, Schuh H (2012) The new Vienna VLBI Software VieVS. In: Proceedings of the 2009 IAG symposium, Buenos Aires, Argentina, International Association of Geodesy Symposia, vol 136, 31 August-4 September, pp 1007-1011
- Clark T, Corey B, Davis J, Elgered G, Herring T, Hinteregger H, Knight C, Levine J, Lundqvist G, Ma C, Nesman E, Phillips R, Rogers AE, Ronnang B, Ryan J, Schupler B, Shaffer D, Shapiro I, Vandenberg N, Webber J, Whitnety A (1985) Precision Geodesy Using the Mark-III Very-Long-Baseline Interferometer System. *ITGRS GE-23*: 438-449

- Haas R, Hobiger T, Kurihara S, Hara T (2017) Ultra-rapid earth rotation determination with VLBI during CONT11 and CONT14. *J Geod* 91: 831-837
- Hase H, Behrend D, Ma C, Petrachenko B, Schuh H, Whitney A (2012) The Emerging VGOS Network of the IVS. In: *IVS 2012 General Meeting Proceedings*, pp 8-12.
- Hellerschmied A, and Plank L, and McCallum JN, Sun J, Lovell J, Böhm J (2017) Observations of the APOD satellite with the AuScope VLBI network. In: *EGU General Assembly Conference Abstracts* 19: 14304
- Hobiger T, Kondo T, Schuh H (2006) Very long baseline interferometry as a tool to probe the ionosphere. *Ra Sc* 41: 10.
- IERS (2017) IERS Bulletin A (rapid EOP data and predictions). In: *IERS News Bulletins*. <https://datacenter.iers.org/web/guest/eop/-/somos/5Rgv/latest/6>
- Iles EJ, McCallum L, Lovell JEJ, McCallum JN (2017) Automated and Dynamic Scheduling for Geodetic VLBI - A Simulation Study for AuScope and Global Networks. *Ad Sp R* 61: 962-973.
- Krásná H, Böhm J, Schuh H (2013) Tidal Love and Shida numbers estimated by geodetic VLBI. *J Geo* 70: 21-27.
- Kurihara S, Lovell J, Cho J, Gulyaev S, Shu F, Kawabata R (2014) Foundation of the Asia-Oceania VLBI Group for Geodesy and Astrometry. In: *IVS 2014 Annual Report*, pp 20-25.

- Lovell J, McCallum J, Reid P, McCulloch P, Baynes B, Dickey J, Shabala S, Watson C, Titov O, Ruddick R, Twilley R, Reynolds C, Tingay S, Shield P, Adada R, Ellingsen S, Morgan J, Bignall H (2013) The AuScope geodetic VLBI array. *J Geod* 87: 527-538
- Lovell JEJ, McCallum JN, Shabala S, Plank L, Böhm J, Mayer D, Sun J (2014) Dynamic Observing in the VGOS Era. In: *IVS 2014 General Meeting Proceedings*, pp 43-47.
- Lovell JEJ, Plank L, McCallum JN, Shabala S, Mayer D (2016) Prototyping automation and dynamic observing with the AuScope array. In: *IVS 2016 general meeting proceedings*, pp 92-95.
- Lovell JEJ, McCallum L, McCallum JN, Iles EJ, Quick J (2017) A Year of Dynamic Observing. In: *23rd EVGA Working Meeting & 18th IVS Analysis Workshop* (in pres)
- Ma C (1999) The celestial reference frame. In: Vandenberg N, Baver K (eds) *IVS 1999 Annual Report*, pp 18-22
- Malkin Z (2009) On comparison of the Earth orientation parameters obtained from different VLBI networks and observing programs. *J Geod* 83: 547-556
- Matveenko LI, Kardashev NS, Sholomitskii GB (1965) Large base-line radio interferometers. *Sov Radiophy* 4: 461-463.
- NCRIS (2006) National Collaborative Research Infrastructure Strategy (NCRIS). <http://www.innovation.gov.au/Science/ResearchInfrastructure/Pages/NCRIS.aspx>

- Neidhardt A, Ettl M, Rottmann H, Plötz C, Mühlbauer M, Hase H, Alef W, Sobarzo S, Herrera C, Himwich E (2010) E-control: First public release of remote control software for VLBI telescopes. In: Behrend D, Baver K (eds) IVS 2010 General Meeting Proceedings, NASA/CP 2010-215864, pp 439-443
- Nilsson T, Haas R, Elgered G (2007) Simulations of atmospheric path delays using turbulence models. In: Böhm J, Pany A, Schuh H (eds) Proceedings of the 18th European VLBI for Geodesy and Astrometry Work Meeting, 12-13 April, ISSN 1811-8380, pp 175-180
- Nothnagel A, Artz T, Behrend D, Malkin Z (2016a) International VLBI Service for Geodesy and Astrometry. *J Geod* 91: 711-721.
- Nothnagel A, Behrend D (2016b) Report of the IAG: International VLBI Service for Geodesy and Astrometry (IVS). *Int VLBI Serv Geod Astrom.*
- Nothnagel A, Behrend D, Bertarini A, Charlot P, Combrinck L, Gipson J, Himwich E, Haas R, Ipatov A, Kawabata R, Lovell JEJ, Ma C Niell A, Petrachenko B, Schüler T, Wang G (2016) Strategic Plan of the IVS for the Period 2016-2025. *Int VLBI Serv Geod Astrom.*
- Pany A, Böhm J, MacMillan DS, Schuh H, Nilsson T, Wresnik J (2010) Monte Carlo simulations of the impact of troposphere, clock and measurement errors on the repeatability of VLBI positions. *J Geod* 85: 39-50.
- Petrachenko W, Niell A, Corey B, Behrend D, Schuh H, Wresnik J (2009) VLBI2010: next generation VLBI system for Geodesy and Astrometry. In: Proceedings of 2009 IAG symposium, Buenos Aires, Argentina, Inter-

national Association of Geodesy Symposia, vol 136, 31 August-4 September, pp 999-1006

Petrachenko B, Behrend D, Hase H, Ma C, Niell A, Nothnagel A, Zhang X (2014) VGOS Observing Plan. IVS.

Petrov L, Gordon D, Gipson J, MacMillan D, Ma C, Fomalont E, Craig Walker R, Carabajal C (2009) Precise geodesy with the very long baseline array. *J Geod* 83: 859-876.

Plank L, Lovell JEJ, McCallum JN, Mayer D, Reynolds C, Quick J, Weston S, Titov O, Shabala S, Böhm J, Natusch T, Nickola M, Gulyaev S (2017) The AUSTRAL VLBI observing program. *J Geod* 91: 803-817

Robertson DS (1991) Geophysical applications of very-long-baseline interferometry. *Rev Mod Phys* 63: 899-918.

Schartner M, Böhm J, Mayer D, McCallum L, Hellerschmied A (2017) Recent developments in scheduling with VieVS. In: 23rd EVGA Working Meeting & 18th IVS Analysis Workshop (in pres)

Schlüter W, Behrend D (2007) The International VLBI Service for Geodesy and Astrometry (IVS): current capabilities and future prospects. *J Geod* 81: 379-387.

Schuh H, Behrend D (2012) VLBI: a fascinating technique for geodesy and astrometry. *J Geo* 61: 68-80.

Shapiro II, Knight CA (1970) Geophysical applications of long-baseline radio interferometry. In: Mansinha L, Smylie DE, Beck A (eds) *Earthquake*

displacement field and the rotation of the Earth. Reidel, Dordrecht, pp 284-301

Sun J, Böhm J, Nilsson T, Krásná H, Böhm S, Schuh H (2014) New VLBI2010 scheduling strategies and implications on the terrestrial reference frames. J Geod 88: 449-461.

Thompson AR, Moran JM, Swenson GW (1987) Interferometry and synthesis in radio astronomy. John Wiley & Sons Inc, USA, pp 247-313

Titov O (2007) Effect of the selection of reference radio sources on geodetic estimates from VLBI observations. J Geod 81: 455-468.

UN (2015) A global geodetic reference frame for sustainable development. United Nations General Assembly 69/266. <http://ggim.un.org/knowledgebase/KnowledgebaseArticle50334.aspx>

Walker RC (1989) Very Long Baseline Interferometry I: Principles and Practices. In: Perley RA, Schwab FR, Bridle AH (eds) A Collection of Lectures from the Third NRAO Synthesis Imaging Summer School: Synthesis Imaging in Radio Astronomy. PASP 6: 439-443

Whitney AR (2000) How Do VLBI Correlators Work? In: First IVS General Meeting Proceedings.

Appendix A

Summary Paper - Manuscript

Published As:

Iles EJ, McCallum L, Lovell JEJ, McCallum JN (2017) Automated and Dynamic Scheduling for Geodetic VLBI - A Simulation Study for AuScope and Global Networks. *Ad Sp R* 61: 962-973

See attached for statement of co-authorship.

This article has been
removed for copyright or
proprietary reasons.